# INTERIM REPORT

Application of Statistically Based Site Characterization Tools to Victorville Precision Bombing Ranges Y and 15 for the ESTCP Wide Area Assessment Demonstration

ESTCP Project MM-0325

OCTOBER 2007

J.B. Roberts Hathaway
S. McKenna
**Sandia National Laboratories**

B.Pulsipher
**United States Geological Survey**

**ESTCP**

Environmental Security Technology
Certification Program

| | | | |
|---|---|---|---|
| **Report Documentation Page** | | | *Form Approved* <br> *OMB No. 0704-0188* |

Public reporting burden for the collection of information is estimated to average 1 hour per response, including the time for reviewing instructions, searching existing data sources, gathering and maintaining the data needed, and completing and reviewing the collection of information. Send comments regarding this burden estimate or any other aspect of this collection of information, including suggestions for reducing this burden, to Washington Headquarters Services, Directorate for Information Operations and Reports, 1215 Jefferson Davis Highway, Suite 1204, Arlington VA 22202-4302. Respondents should be aware that notwithstanding any other provision of law, no person shall be subject to a penalty for failing to comply with a collection of information if it does not display a currently valid OMB control number.

| 1. REPORT DATE <br> **OCT 2007** | 2. REPORT TYPE | 3. DATES COVERED <br> **00-00-2007 to 00-00-2007** | |
|---|---|---|---|

| 4. TITLE AND SUBTITLE <br> **Application of Statistically Based Site Characterization Tools to Victorville Precision Bombing Ranges Y and 15 for the ESTCP Wide Area Assessment Demonstration** | 5a. CONTRACT NUMBER |
|---|---|
| | 5b. GRANT NUMBER |
| | 5c. PROGRAM ELEMENT NUMBER |
| 6. AUTHOR(S) | 5d. PROJECT NUMBER |
| | 5e. TASK NUMBER |
| | 5f. WORK UNIT NUMBER |
| 7. PERFORMING ORGANIZATION NAME(S) AND ADDRESS(ES) <br> **Sandia National Laboratories,PO Box 5800,Albuquerque,NM,87185** | 8. PERFORMING ORGANIZATION REPORT NUMBER |
| 9. SPONSORING/MONITORING AGENCY NAME(S) AND ADDRESS(ES) | 10. SPONSOR/MONITOR'S ACRONYM(S) |
| | 11. SPONSOR/MONITOR'S REPORT NUMBER(S) |

12. DISTRIBUTION/AVAILABILITY STATEMENT <br> **Approved for public release; distribution unlimited**

13. SUPPLEMENTARY NOTES

14. ABSTRACT

15. SUBJECT TERMS

| 16. SECURITY CLASSIFICATION OF: | | | 17. LIMITATION OF ABSTRACT | 18. NUMBER OF PAGES | 19a. NAME OF RESPONSIBLE PERSON |
|---|---|---|---|---|---|
| a. REPORT <br> **unclassified** | b. ABSTRACT <br> **unclassified** | c. THIS PAGE <br> **unclassified** | **Same as Report (SAR)** | **64** | |

**Standard Form 298 (Rev. 8-98)** <br> Prescribed by ANSI Std Z39-18

# Contents

# Figures

# Tables

# 1. Introduction

Efficient characterization and remediation of sites potentially contaminated with unexploded ordnance (UXO) remain a high priority for the U.S. Department of Defense (DoD). Recent estimates of the amount of land that is potentially contaminated with UXO are as high as 10 million acres (4 million hectares). This total land area is comprised of as many as several thousand individual sites. Characterization efforts to date have shown that at a typical site the UXO contamination is concentrated in a small portion of the site area, often only 10 to 20 percent of the entire area. Therefore, efficient site characterization should be focused on identifying the location and extent of these smaller areas within a site. Toward this goal, Pacific Northwest National Laboratory (PNNL) and Sandia National Laboratories (SNL) have developed efficient and defensible, statistically based approaches for UXO site characterization.

The Environmental Security Technology Certification Program (ESTCP) established several demonstrations of UXO site characterization technologies under a Wide Area Assessment (WAA) Project. This report focuses on the application and performance of statistically based tools to the Victorville Precision Bombing Range located near Victorville, California. PNNL and SNL have developed statistical algorithms to create transect designs based on desired Data Quality Objectives (DQO) and then identify potential target areas based on the surveyed transects. The transect design tools provide a statistically defensible method that uses transect survey data for only a small proportion of the total study area (i.e., 1 to 3 percent) to identify target areas of a specific size, shape, and anomaly density. Target area density estimates, probability estimates, and density flagging routines are applied after the data are gathered from the established transect design to separate potential target areas from areas that require no further remediation. These tools, combined with the other components of the WAA Project, can be used to correctly and efficiently aid in the investigation of formerly used defense sites.

This report documents the application of these statistically based site characterization tools to the Victorville Precision Bombing Range as part of the ESTCP WAA Project. Specifically, these tools are used to accomplish 1) geophysical transect design to locate potential target areas with agreed upon DQOs, 2) anomaly density estimation across the site using the geophysical data collected along the transect design, and 3) target area boundary delineation.

# 2. Victorville WAA Site Information and Munitions Use

The former Victorville Precision Bombing Range is located in San Bernardino County, California, and lies to the east of Victorville. The site is located in a valley between two northwest-southeast trending bedrock ridges with the bed of Means Dry Lake located in the valley. The Victorville WAA study area contains Demolition Bombing Target "Y" (VV-Y), Precision Bombing Target 15 (VV-15), and the surrounding buffer area that is approximately 42 miles southeast of Victorville. This WAA study area (shown in Figure 1) is a part of the larger Victorville Precision Bombing Range.

Target VV-Y was mainly used for practice with demolition bombs of sizes ranging from 100 to 2000 pounds. However, the conceptual site model (CSM) and the archive search report (ASR) infer that the 100-pound bombs were the most commonly used munition. A walk-over of the southern target located in VV-15 showed evidence of 100-pound practice bombs with no visible craters present. Both the CSM and the ASR suggest 100-pound practice bombs were the primary, if not only, munition used in VV-15.

This WAA study involved high-altitude, airborne lidar and ortho-photography platforms, helicopter mounted magnetometer surveys, and ground-based magnetometer surveys augmented with electromagnetic induction (EMI) surveys. This report summarizes the ground-based transect design approach and the statistical evaluation of those transect survey results, and illustrates how information from the aerial imagery helps explain the findings from the ground-based transect analyses.

## 3. Transect Design and Analysis Approach

Visual Sample Plan (VSP) is a statistical sampling software package designed by PNNL through funding from multiple government agencies to provide site investigators an easy-to-use, defensible method of gathering and analyzing their respective data. Through funding from the Strategic Environmental Research and Development Program (SERDP) and ESTCP, VSP contains a transect-sampling module for transect design and methods for analyzing the gathered transect data to identify and delineate areas of high anomaly density. PNNL is also integrating SNL's geostatistical analysis algorithms into VSP. These algorithms are used and demonstrated in this document for target area identification, delineation, and density estimation.
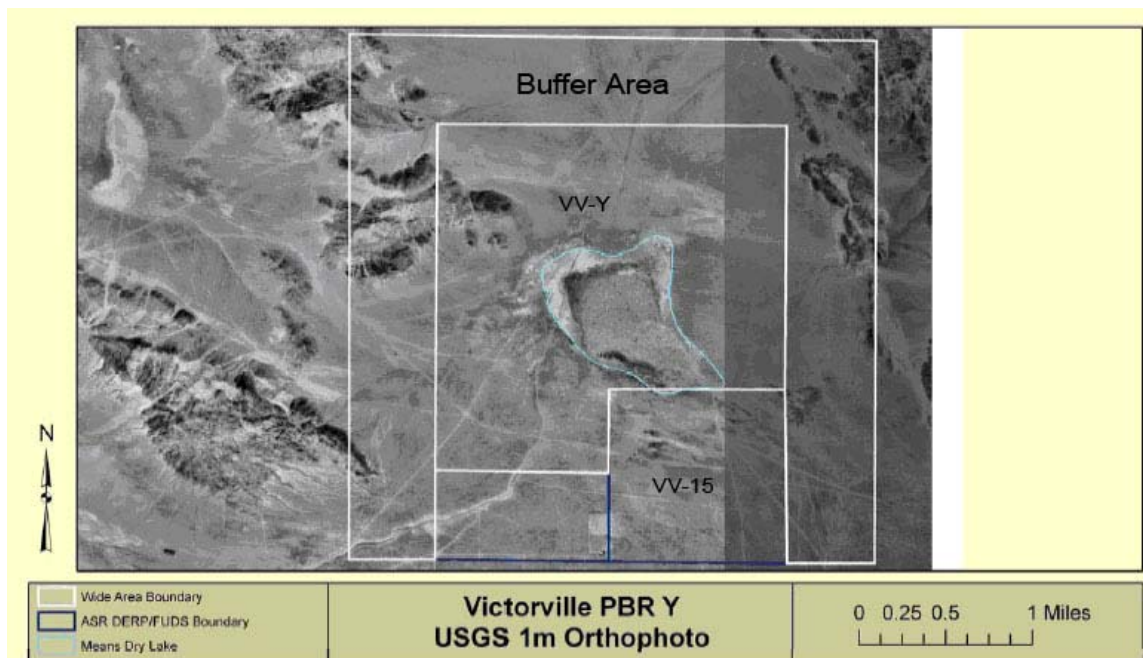


**Figure 1.** Image of the Victorville WAA site. The white perimeter lines represent the different impact and buffer areas located within the site and other points of interest have been labeled in the picture.

## 3.1. Transect Design Approach

Given specific design parameters, VSP will compute the required spacing of transects to achieve the specified probability of traversing and detecting the critical target zone if it exists, display the proposed transects on the site map, and output the coordinates of the proposed transects. The user can also conduct a sensitivity analysis by evaluating the effects of changing the input parameters and managing the required DQOs. These methods and tools allow the project team to balance DQO goals against costs and other site constraints. Figure 2 shows the design dialogues in VSP and an example of inputs that create graphs similar to the graphs displayed in Section 4.1 and 4.5
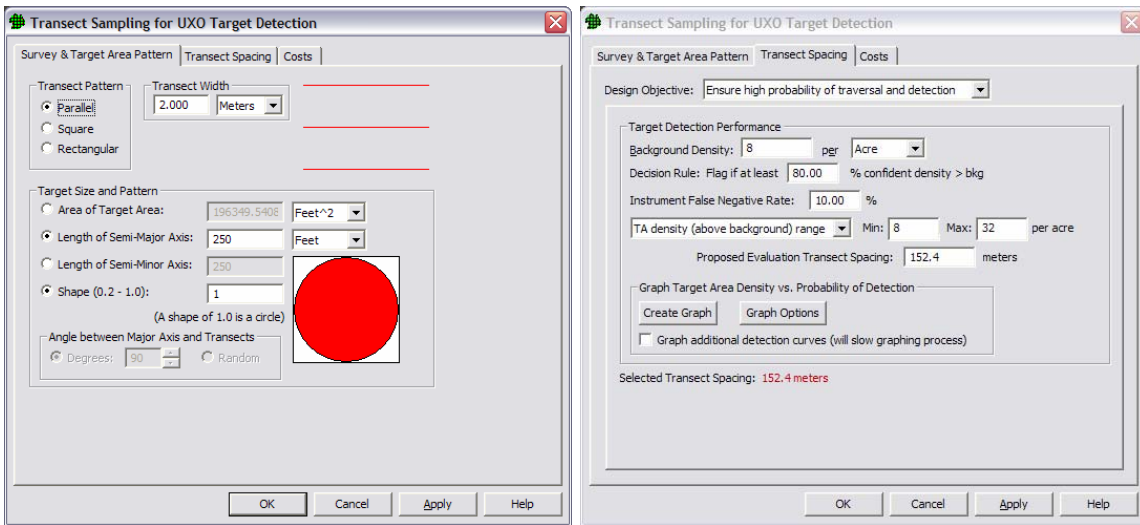


**Figure 2.** The design dialogues in VSP allow the user to input transect pattern, width and target area size, shape, and orientation (left). Probability of detection curves can be displayed based on inputs and site assumptions (right).

## 3.2. Target Area Identification Approach

After the sample area is identified and the necessary geophysical survey results have been imported into VSP the user can then analyze the data. VSP provides two dialogs for analyzing the spatial data. The first dialog, "Locate and Mark UXO Target Areas Based on Elevated Transect Anomaly Density," identifies those locations within the transects that are identified as being high density (i.e., high number of anomalies within a specified amount of the surveyed transect area). The second dialog, "Geostatistical Mapping of Anomaly Densities," uses the anomaly densities along the transects to create a map of estimated densities over the entire site.

### 3.2.1. Locate and Mark UXO Target Areas Based on Elevated Transect Anomaly Density

To identify high-density areas along transects, VSP passes a window over segments of the site and calculates the anomaly density for each segment. The window diameter specifies the size of the circular area over which the average density is computed. Figure 3 shows where the window diameter is selected using the VSP analysis dialog. Figure 4 provides an example of how the window diameter is used to calculate transect grid densities. The window diameter defines the size of a centered circular window (orange and blue circles in Figure 4), which moves every one-sixth of the selected diameter and uses the anomaly count with the transect area within the window to calculate a density assigned to the central transect grid (orange and blue boxes in Figure 4) centered in the window. The green dots in Figure 4 represent the identified anomalies within the two surveyed transects. This figure provides an example of two of the multiple transect grid densities that would be calculated on these transects.

The selection of an appropriate window diameter is dependent on the size of the target area of interest (AOI), transect width, and spacing between transects. The optimum window diameter is one that has sufficient traversed area within the window without including such a large area that potential high-density areas can be masked by the surrounding low-density areas in the window. The blue window in Figure 5 provides an example of a window that is too large. If the window diameter is too small (red window in Figure 5), then the limited amount of traversed area within the window is not sufficient to make accurate transect grid density estimates. Within these two extremes, there are often many different window diameters that would be appropriate. As a general rule, the window diameter should be less than the diameter of the target area of interest and no smaller than the spacing between the original transect design. Selecting the appropriate window diameter for each specific site analysis currently is left to the user.

This moving window algorithm is used to create a histogram of the anomaly densities across the site (see Figure 6 and Figure 7). In cases where the anomaly density distribution of the site is unknown and there is no reliable historical data to use as an estimate, a histogram of the density calculations for the entire site can provide a good understanding of the anomaly density distribution. The primary purpose for this histogram is to help select a critical density above which areas will be flagged by distinguishing between high-density target areas and lower-density background values.
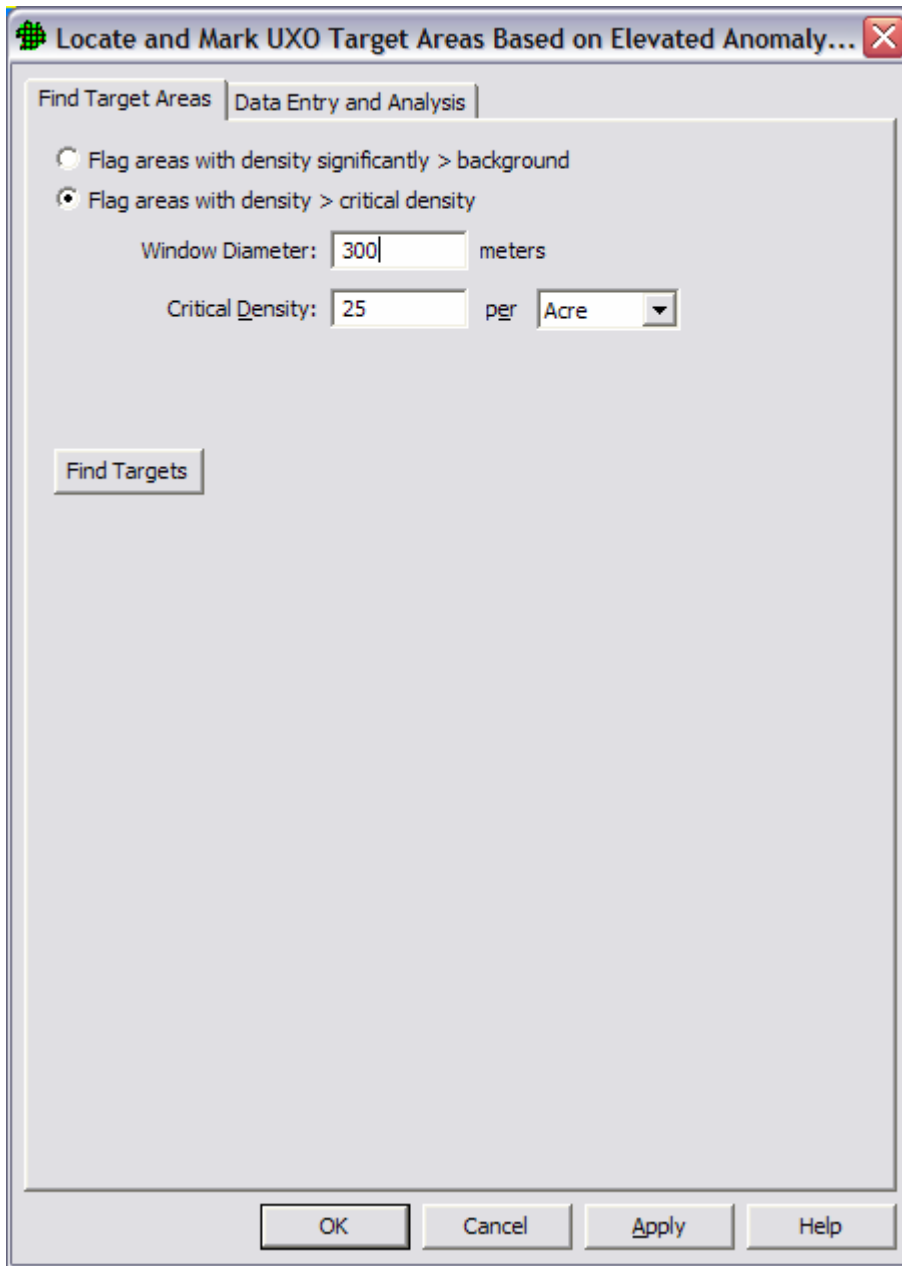
**Figure 3.** "Locate and Mark UXO Target Areas Based on Elevated Transect Anomaly Density" dialog in which the window diameter is specified.
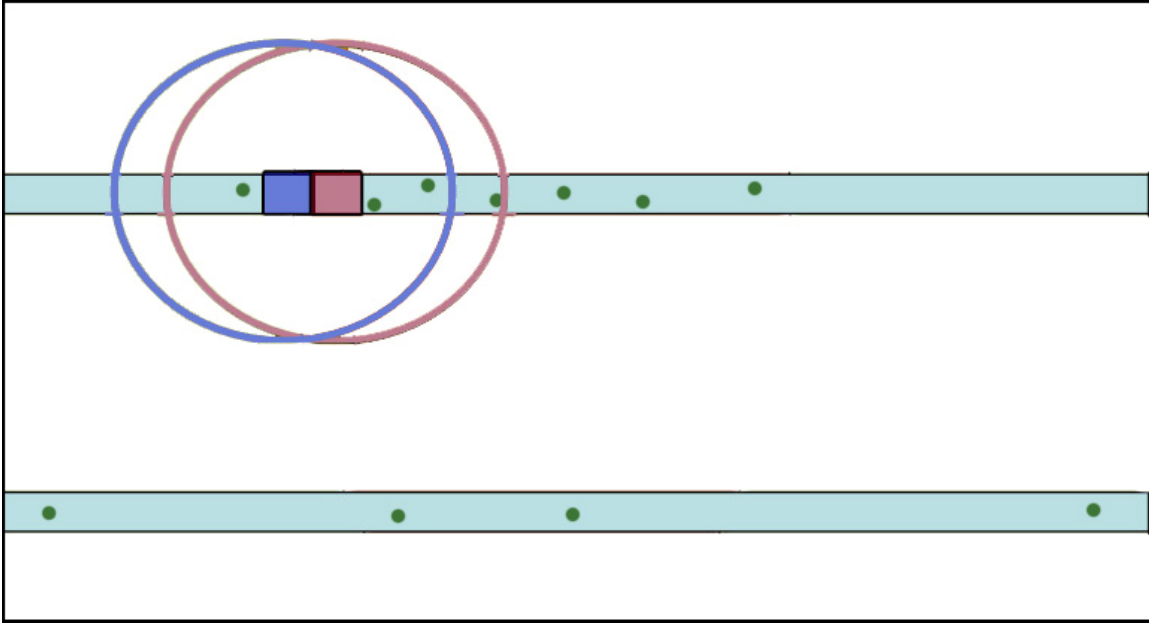
**Figure 4.** Depiction of the window density calculation process used to identify high density regions within a site.
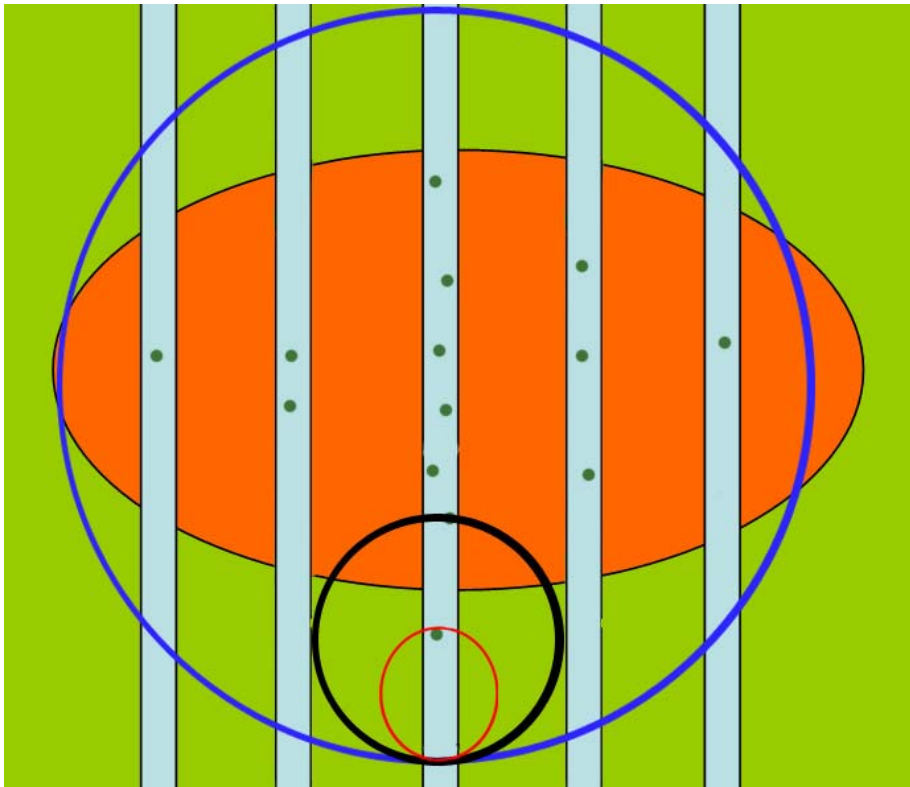


**Figure 5.** Example of different window sizes and how they would encompass the transect lines.

The circular window size used in this report was set to a 300-m-diameter window that is similar to the assumed 1000-ft-diameter target area. Figure 6 and Figure 7 are histograms of the site densities from the conservative with additional transect design (described below). Figure 7 shows the same densities as Figure 6, but the frequency axis is distorted logarithmically to accentuate the lower count bins. This site had multiple high-density areas of which each had a unique average density. Using this window size, different critical densities were considered and an evaluation of the anomaly data suggests that critical densities between 45 and 65 anomalies per acre identifies the potential transition region between densities associated with background and those associated with possible target areas. The critical density of 53 anomalies per acre (ApA) is within this region and was used to identify all the high-density areas on the site.
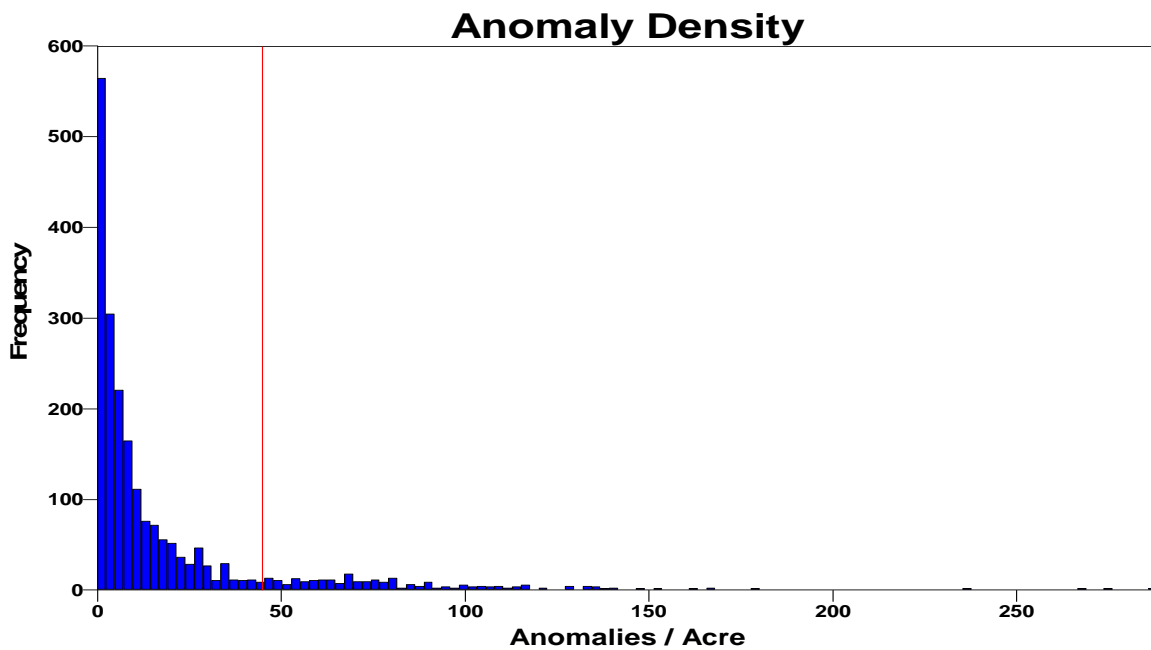


**Figure 6.** Histogram produced using the "Find UXO Target Areas" target-area-identification dialog in VSP of the calculated site densities from a survey performed at WAA site located near Victorville, California. The window diameter was 300 m.
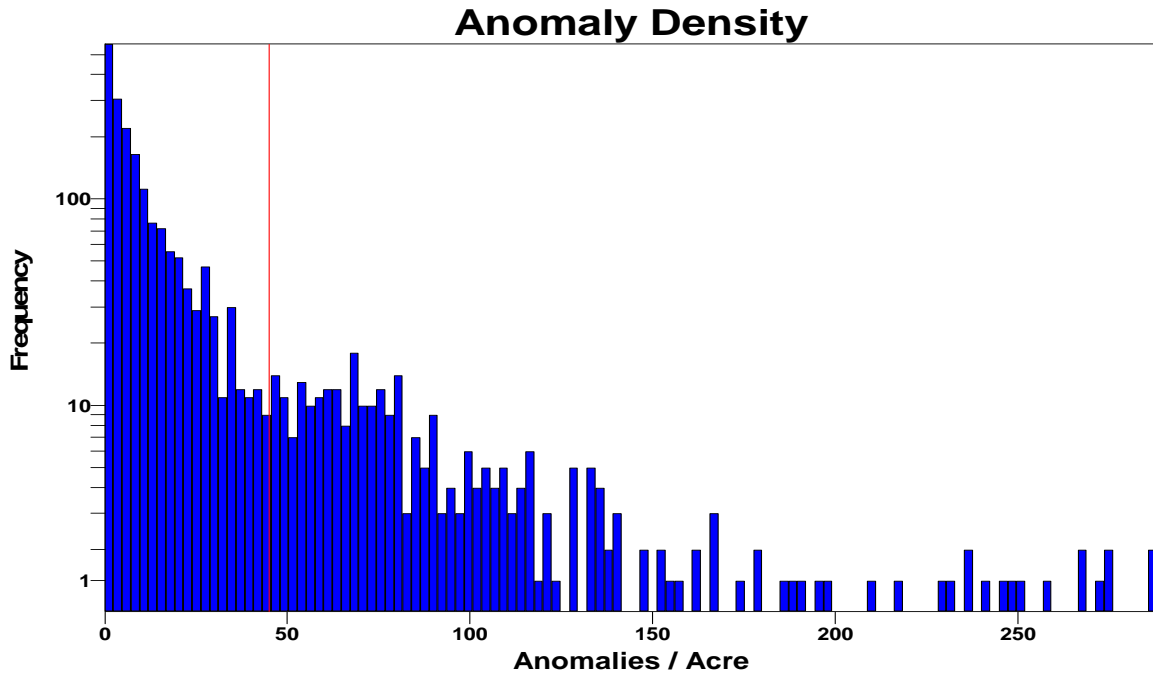
**Figure 7.** Histogram produced from VSP using the same data from Figure 6, but the frequency axis is distorted to accentuate the bins with low counts.

### 3.2.2. Geostatistical Kriging for Identification, Delineation, and Estimation of High Anomaly Density Areas

Kriging refers to a category of general least-squares regression techniques used for estimating unknown values. It typically is used to estimate values at unsampled locations for some spatially varying characteristic. Kriging provides an unbiased estimate in that it attempts to have the residual errors sum to zero. It also attempts to simultaneously minimize the error variance of the estimates. The goal of the kriging estimation process as applied here is to identify areas with high concentrations of magnetic anomalies. These areas can then be delineated as areas of interest that may represent former range target areas.

Kriging estimation relies on the spatial autocorrelation of the characteristic being sampled. Spatial autocorrelation refers to the level of similarity of data values from different locations in the study area. The autocorrelation of the characteristic being estimated is a key factor in the geostatistical estimation and must be modeled as part of the estimation procedure. Modeling of the autocorrelation is typically performed using semivariograms that depict how the variance in the data set changes with increasing separation distance between the data locations. These semivariograms are an integral part of the kriging process, which is used to interpolate values for unsampled locations using surrounding data points.

Geostatistical estimation using kriging techniques was used to provide estimates of site properties away from the transect locations to unsurveyed locations of the site domain. Kriging estimates of two site properties were developed from the geophysical transect data. A probabilistic estimate of being within a target area was developed using Indicator Kriging (IK). Indicator kriging enables direct mapping of the probability of exceeding a critical magnetic anomaly density threshold across the site. The resulting probability map defines the probability of being within a target area and can be used as part of the target identification and delineation process. Target areas can be defined as those regions where the probability of being within the target exceeds a probability contour (e.g., 5 percent) as specified by the site characterization team. The input data for the IK was composed of an indicator variable developed from the geophysical transect data. This indicator variable had a value of "1" where the magnetic anomaly density of the transect was at or above the defined threshold, and a value of "0" where the density was below the threshold.

The second site property estimated using kriging techniques was the magnetic anomaly density distribution. In this case, the estimated magnetic anomaly density at every location is the mean value of a Poisson distribution defining the number of anomalies within an area. Density estimation provides additional information for target area boundary delineation. A density contour is selected and areas of the site where the estimated density exceeds this contour are defined as being within the target area. While this target area delineation approach is more straightforward than the probability mapping approach, it is a deterministic approach and does not allow the decision maker any direct consideration of reliability in setting the extent of the target boundary. Magnetic anomaly density estimates were developed using the Ordinary Kriging (OK) algorithm.

As part of data pre-processing prior to geostatistical analyses (kriging), an averaging procedure was applied to the raw magnetic anomaly location data. This procedure is similar to the moving window approach used within the VSP flagging routines, but operates on a grid-cell basis. This process operates by computing the average anomaly density for each grid cell crossed by a sampling transect. Average density values are only computed for those cells actually crossed by a sampling transect as defined by the course-over-ground data provided by the geophysical survey team.

The anomaly density average is computed using a user specified rectangular window around the cell of interest. Typically this window has its greatest dimension parallel to the transect direction. The average anomaly density is computed using the number of anomalies and total sampled area falling within the averaging window. The resulting anomaly density distribution is smoother than the original raw or unsmoothed magnetic anomaly data. The smoothed, more continuous grid cell values of anomaly densities resulting from this process then are used in the subsequent kriging estimates. All anomaly density averaging used square grid cells 20 m in each dimension. This is the same grid cell size employed in the subsequent kriging analyses. For all the kriging estimations presented in this report, an averaging window of 300 m in the X direction (east-west) and 100 m in the Y direction (north-south) was used. The window size in the X direction (parallel to the majority of transects) was chosen to be similar to the expected

target size of 1000 feet (305 m).  The Y direction window size was chosen to be large enough to include field sampling deviations from the original straight-line transect design, but small enough to not include adjacent transects.

# 4.  Victorville WAA Transect Design and Target Area Identification

The Victorville demonstration site differed from the two CSM models for the Pueblo and Kirtland sites conducted previously for the WAA Project.  For the Victorville site, one conservative transect design was developed during a joint meeting of regulators and ESTCP WAA Project members and then these transects were acquired all at once by the survey team.   After these original transects were acquired, a second design was developed which consisted of additional transects requested by PNNL/SNL to improve density estimates in areas where the original transects did not provide adequate information.  A third design, the "sparse design," which was created based on a proposal by PNNL during the transect design meeting, required only half the transects gathered from the conservative design.  Therefore, the sparse design is a subset of the original data gathered from the conservative transects.  Also, a filtered anomaly data scenario was developed that used the second transect design and implemented a filtering algorithm to filter magnetic anomalies from the transect data associated with geologic noise.  Finally, supplemental transects were gathered with a portable EMI system to improve site coverage and anomaly discrimination.  These surveyed transects and the subsequent analysis are presented as a separate analysis.

## 4.1.    Victorville Conservative Transect Design

On January 19, 2006 a transect design site meeting was held in Palm Springs, California.  This meeting had representatives from the U.S. Environmental Protection Agengy (EPA), California Department of Toxic Substances Control, U.S. Army Corps of Engineers, Colorado Department of Public Health and Environment, ESTCP, and PNNL.  Table 1 lists the names of the attendees and their respective organizations.

**Table 1.**  List of Attendees and Their Affiliations

| Names | Organization |
|---|---|
| Anne Andrews | ESTCP |
| Jim Austreng | California Department of Toxic Substances Control |
| Daniel Cordero | California Department of Toxic Substances Control |
| Harry Craig | U.S. EPA Region 10 |
| Alice Gimeno-O'Brien | California Department of Toxic Substances Control |
| John Hathaway | PNNL |
| Katherine Kaye | ESTCP Support (HGL, Inc.) |
| Herb Nelson | NRL |
| Omo Patrick | California Department of Toxic Substances Control |
| Brent Pulsipher | PNNL |
| John Scandura | California Department of Toxic Substances Control |
| Bob Selfridge | U.S. Army Corps of Engineers - Huntsville |
| Larry Sievers | U.S. Army Corps of Engineers |
| Jeff Swanson | Colorado Department of Public Health and Environment |

During the design meeting, several possible transect designs were examined by varying the required confidence, required probability of detection, target sizes, shapes, anomaly densities, and other parameters within VSP. The primary objective was to find and delineate target areas that may be representative of those created by 100-pound demolition and practice bombs. The finalized transect design was the most conservative design examined and resulted in a relatively high probability of detecting both 100-pound practice bombing areas associated with aircraft flying at high altitude and 100-pound, high-explosive (HE)-laden demolition bombing areas resulting from aircraft flying at low altitude (see Figure 8).

The conceptual site model (CSM) for the demolition bombing target area (VV-Y) suggested that the aircraft approached the targets from the south and the variation of the initial impacts could have a major axis of 250 ft and a smaller minor axis. However, the members of the design meeting recognized that the target area assumptions were extremely conservative because they did not account for fragment dispersion around the impact points of the HE munitions. Thus, the size of the target area would be much larger than the 250-ft major axis identified in the CSM.

The 100-pound practice bombs were used on a visible bombing target located in the east-central portion of VV-15, which has a diameter of approximately 180 m. The size of this precision bombing target has similarities to those found on the Pueblo Precision Bombing Range located in southern Colorado. The crater density map of the southern target of the Pueblo site (Figure 9) shows four high-crater-density areas. These high-crater-density areas, which were 150 m to 180 m in diameter, demonstrate the potential range and deflection probable errors for precision bombing use. Given the corroboration of evidence between the two sites, a 500-ft (152.4-m) diameter target area was assumed for the 100-pound practice bomb target area of interest.

Given the two sizes of potential target areas that might exist on this site, VSP was used to explore how the transect sampling requirements and traversal/detection probabilities would be affected for each assumed target area size and shape. Having a high probability of traversal does not necessarily translate into a high probability of detection because detection depends on factors such as the difference between background and target area densities and false negative instrument rates. Given some of the uncertainties surrounding how the fragment dispersions might affect the size of the demolition target areas, the design meeting members concluded that they wanted to take a conservative approach and ensure that they would have a high probability of traversing and detecting a 500-ft-diameter target area. But they also wanted to ensure that at least one transect would traverse a 250 ft diameter target area if it existed. Therefore, VSP was used to develop 2-m-wide transects spaced 78.1 m apart to guarantee a 100 percent probability of traversal for all target areas larger than 250 ft in diameter. This transect spacing was then evaluated to determine the probability of detecting 500-ft-diameter target areas. The achieved detection probability was very high (~0.99) when the target area anomaly density is 8 above the assumed background density as shown in Figure 10. Thus, this 78.1 m spacing was deemed acceptable and very conservative.

All three areas (i.e., VV-Y, VV-15, and Buffer) had the same transect spacing applied to ensure an adequate degree of confidence that no target areas of the assumed size and shape would go undetected in any portion of the study area. A summary of the final design parameters (Table 2), the transect locations (Figure 8), and the statistical power curve showing the probability of detecting a 500-ft circular target area (Figure 10) are shown below.
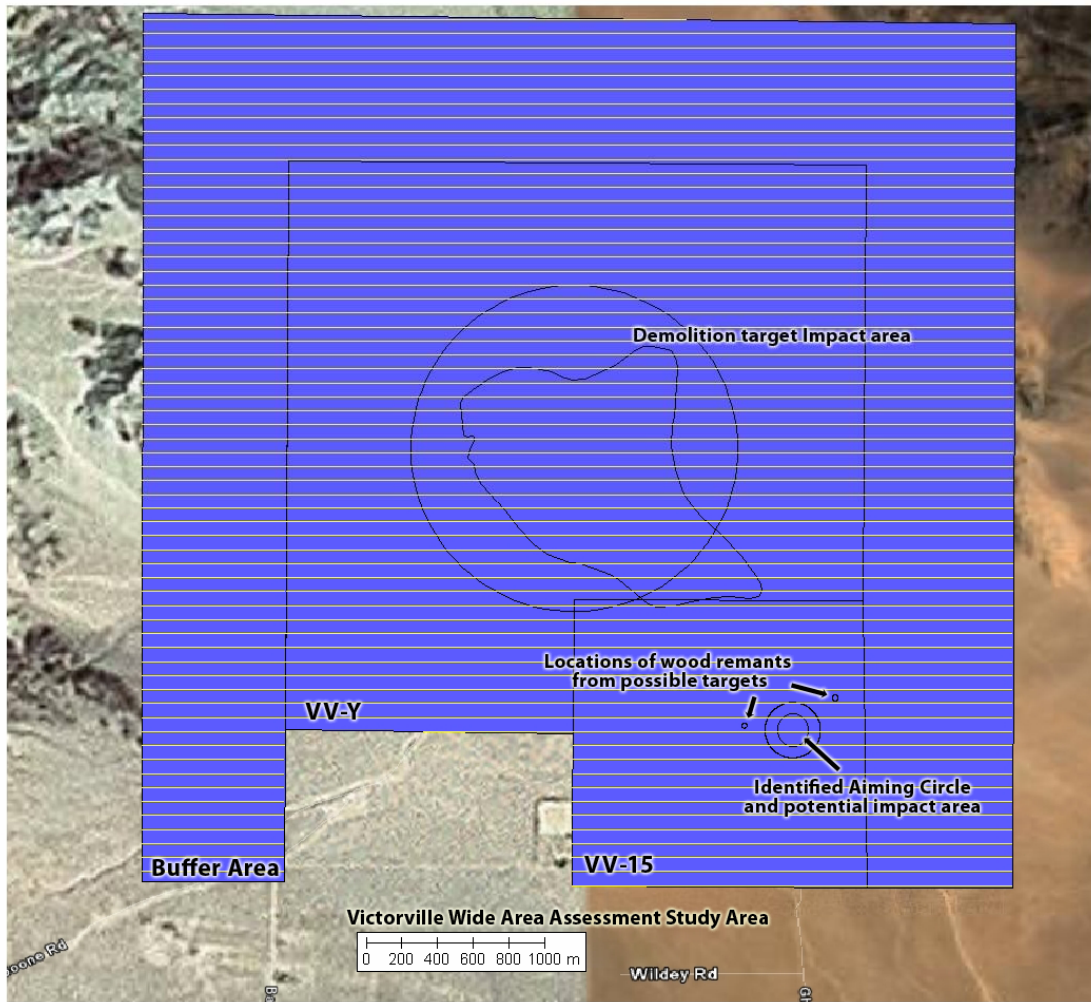


**Figure 8.** Finalized design with 2-m-wide transects spaced 78 m apart on centers assuming a 250- by 125-ft, north-south oriented elliptical target area.
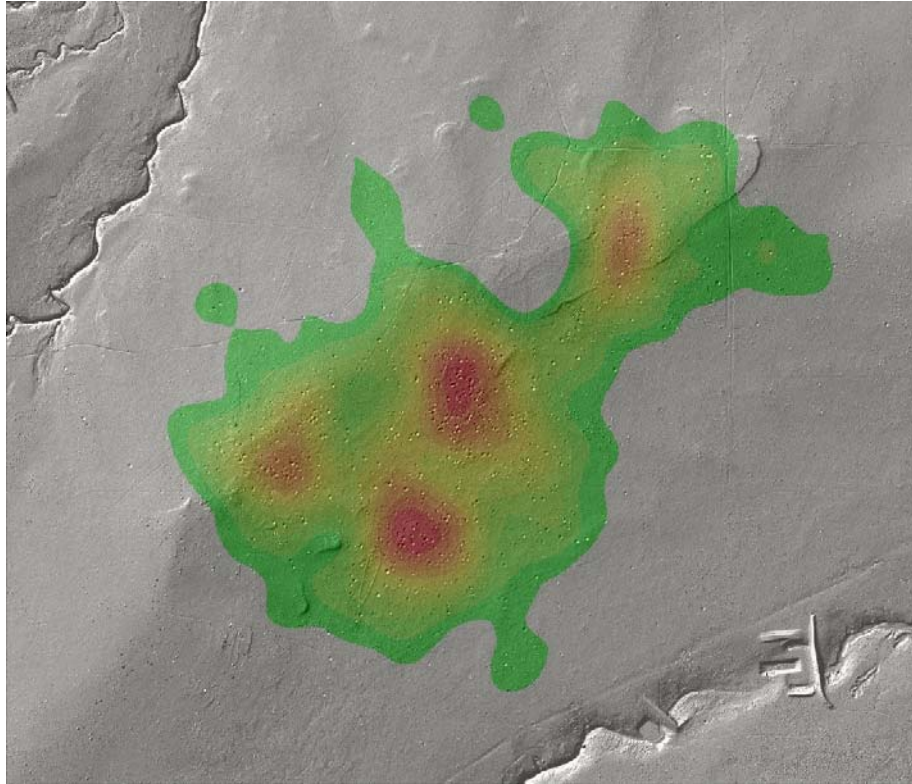
**Figure 9.** Crater density map of the southern target from the Pueblo Precision Bombing Range WAA site. Each of the four red centers represent the high crater density that surrounds each of the four identified ship features located in the lidar images. The area that is contained by the shaded colors from red to orange was used as the approximate size of the impact area for each target. High explosive fragments would spread beyond these identified areas. High crater density areas are 150-180m wide.

**Table 2.** Summary of design parameters and results for the final proposed design.

| | |
|---|---|
| Primary Objective of Design | Detect the presence of a high-density area that has a specified size and shape |
| Diameter of target area of concern | 500 ft |
| Shape of target area of concern | Circular |
| Type of Sampling Design | Parallel Transects |
| Specified sampling area | 22,265,069 m$^2$ |
| Transect width | 2 m |
| Spacing between transects | 76.1 m |
| Spacing between transect centers | 78.1 m |
| Total length of transects | 285877.5 m |
| Area to be surveyed (Area under the transects) | 571755 m$^2$ |
| Percent of sample area covered by transects | 2.57% |
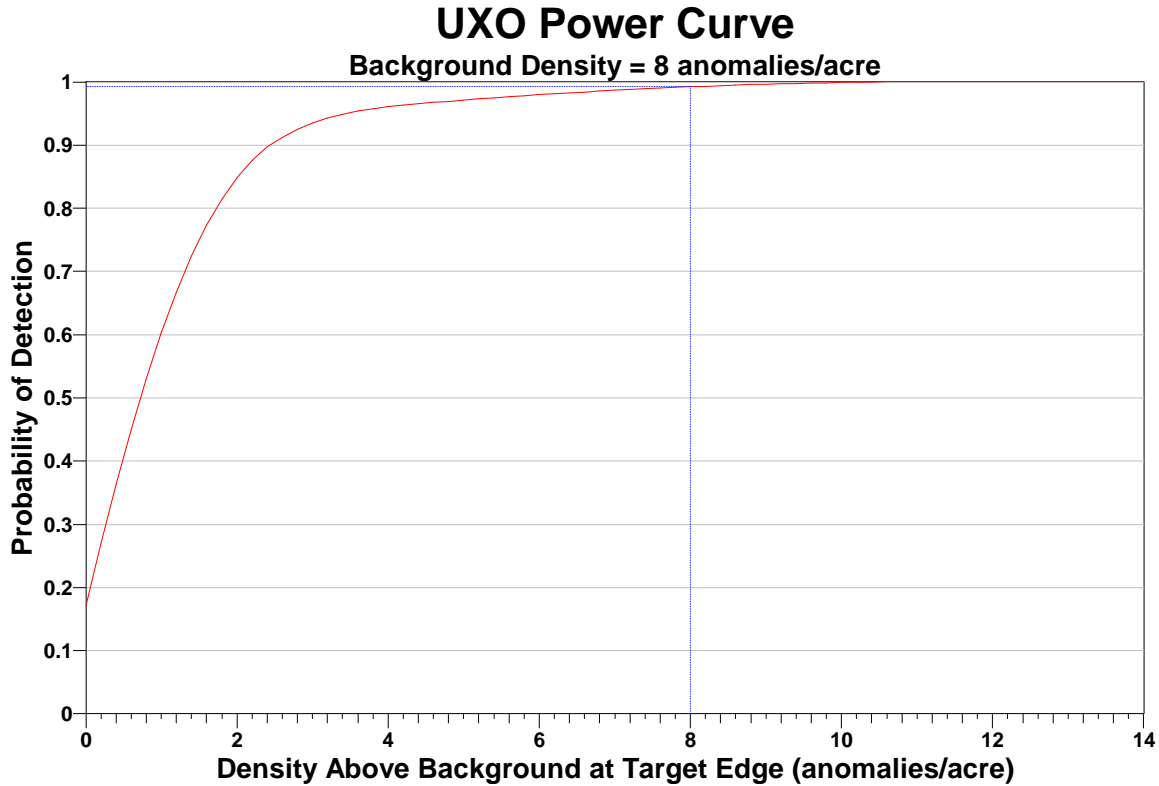
**Figure 10.** Probability of detecting a 500-ft (153-m)-diameter circular target area with 2-m-wide transects spaced 78.1 m apart on centers for various anomaly densities above background. Note that the density above background axis has a much shorter range than Figure 22 to provide a clearer view of the different probabilities of detection and the associated density above background.

## 4.2. Victorville Conservative Transect Design Analysis

The actual course traversed by the geophysical survey team is depicted in Figure 11. This figure shows the generally inaccessible areas (orange regions) where the survey team could not obtain continuous transects with the towed array system. There also were a few locations in the generally accessible areas where surveys were not feasible (gulches, hills, etc.). Within the 3467 accessible acres (yellow area), the survey team covered approximately 85 acres (2.45 percent coverage).
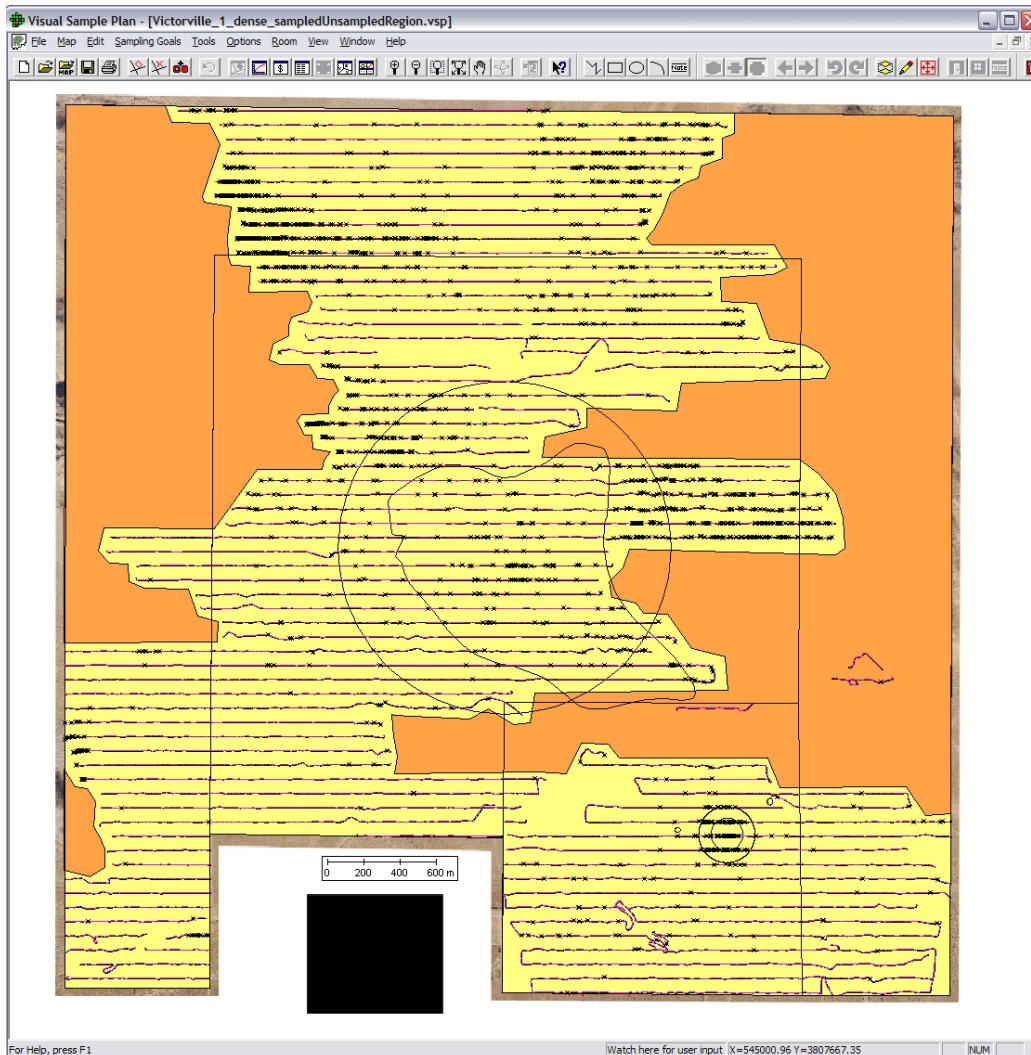
**Figure 11.** Depiction of the actual transects gathered based on the conservative transect design. The black dots represent identified anomalies. The orange region was generally inaccessible to the towed array system.

### 4.2.1. Target Area Identification, Delineation, and Density Estimation

The anomaly data from the transect surveys was used in VSP to flag areas where the anomaly density appeared to be higher than background. Figure 12 shows the flagged areas of high density based on a 300-m-diameter window and a critical density of 53 ApA. The high-density areas identified using a combination of the flagging and kriging routines are labeled as AOIs A through J. Both routines identified all areas except for area J. The flagging routine did not mark this area as shown in Figure 12. Features of interest (i.e., craters) were identified surrounding Area F and the area to the west of Area G. Identified features of interest that may be craters were also located in and around Area D. Figure 13 shows the features of interest from the crater analysis with respect to the AOIs near the dry lake bed. The CSM identified the general regions around Areas G and F as demolition bombing areas and the region around Area I as a practice bombing area. The CSM identified a visible target circle within Area I.

15
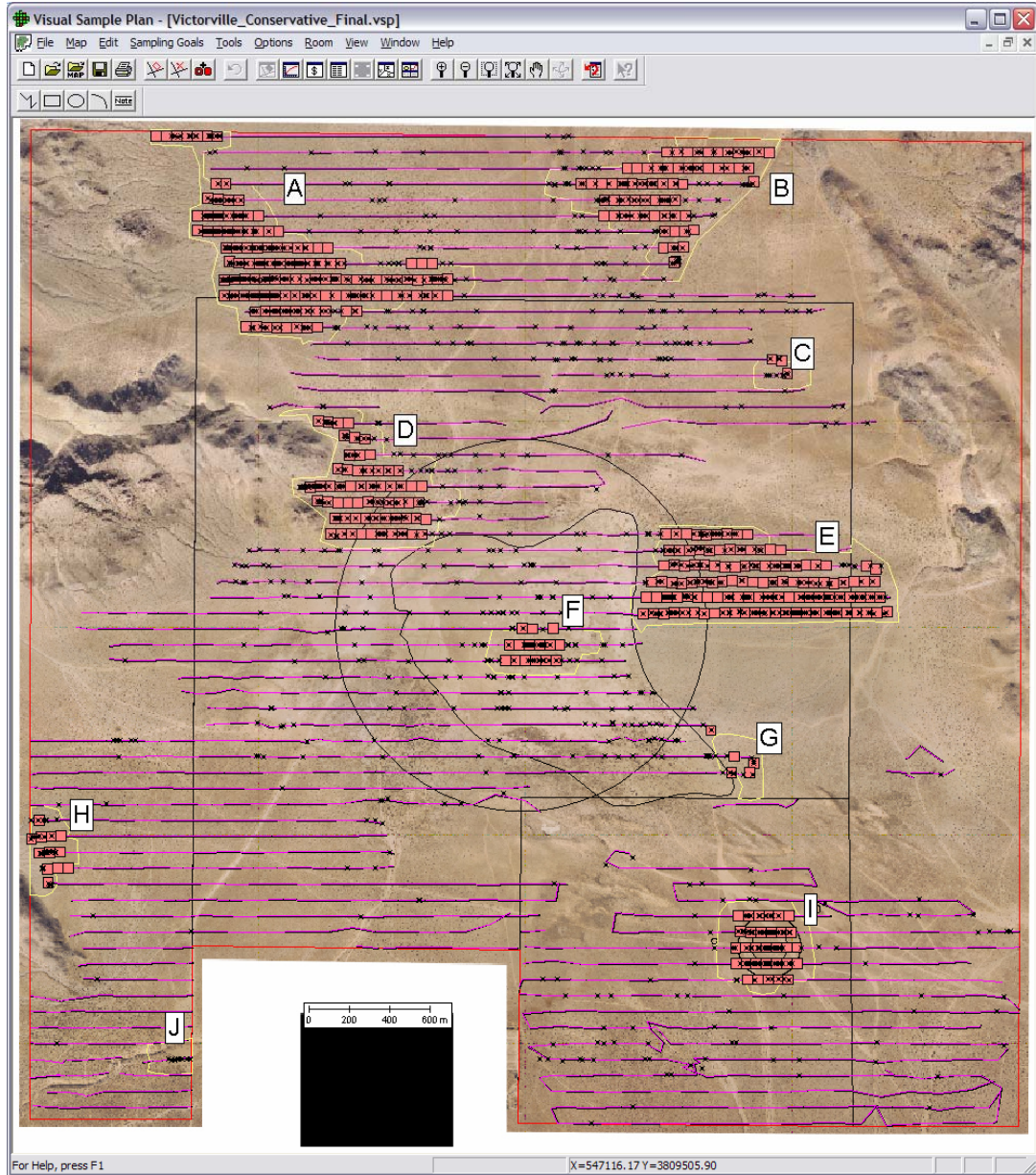
**Figure 12.** Flagged high-density areas of interest for the conservative transect design based on a 300-m-diameter window and a critical density of 53 ApA. High-density area delineations are depicted with yellow lines.
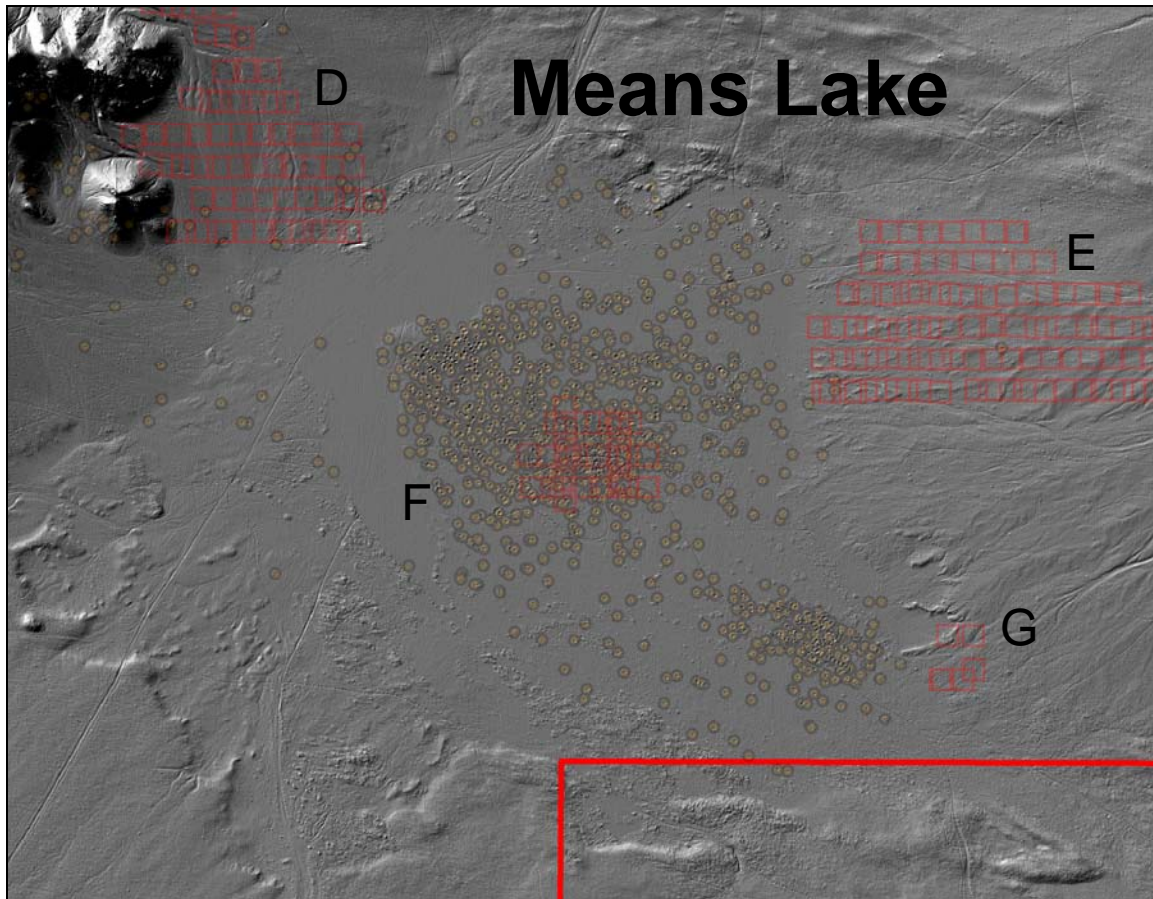
**Figure 13.** Central region of the Victorville WAA study area. Red squares represent flagged areas and orange dots represent features of interest from the crater analysis.

Because of terrain conditions, it was not possible for the field team to collect the full length of the planned geophysical transects for most of the site. Consequently, many of the collected transects do not extend across the full width of the study area, resulting in an irregular outline to the sample area (compare Figure 8 with Figure 12). This irregular outline is reflected in the kriging estimates and the subsequent AOI boundaries. To prevent long-range extrapolation into un-sampled areas, all kriging estimates were clipped to exclude estimated values beyond approximately 40 m from the end of the sampling transects.

The delineation of areas of interest relies primarily on density contrasts in the magnetic anomaly data. The transition from low (background) to high (potential target area) anomaly densities define the margins of the area of interest. For the Victorville site, there are several high-density areas located near the ends of the geophysical transects. The margins of these AOIs are not defined fully because the sample transects end before the anomaly densities return to background values. For these AOIs, the outboard boundaries are based on the limits of the sampled area, and the extent of the high density region is likely beyond what is shown.

Figure 14 shows the indicator kriging probability map for the conservative transect design using an indicator kriging threshold of 53 ApA. Areas with a probability of 0.05 or greater of being above the 53 ApA threshold are indicated by color-filled probability contours. These areas were included as part of the information used in determining the final boundaries for the AOIs.

The indicator kriging threshold value of 53 ApA was chosen based on the spatial pattern resulting from the implementation of different threshold values. The 53 ApA value was selected as the minimum value that did not generate a spatial pattern of the indicator variable, which contained many small isolated clusters in the smoothed anomaly data. The 53 ApA threshold value generated indicator variable spatial patterns with large contiguous areas that would be most like what would be expected for former target areas. The 53 ApA value is approximately 40 ApA above the 12.2 ApA estimated background value for the Victorville site. This background value was estimated from a full-coverage magnetometer survey for a portion of PBR#15 target (ESTCP 2006a).
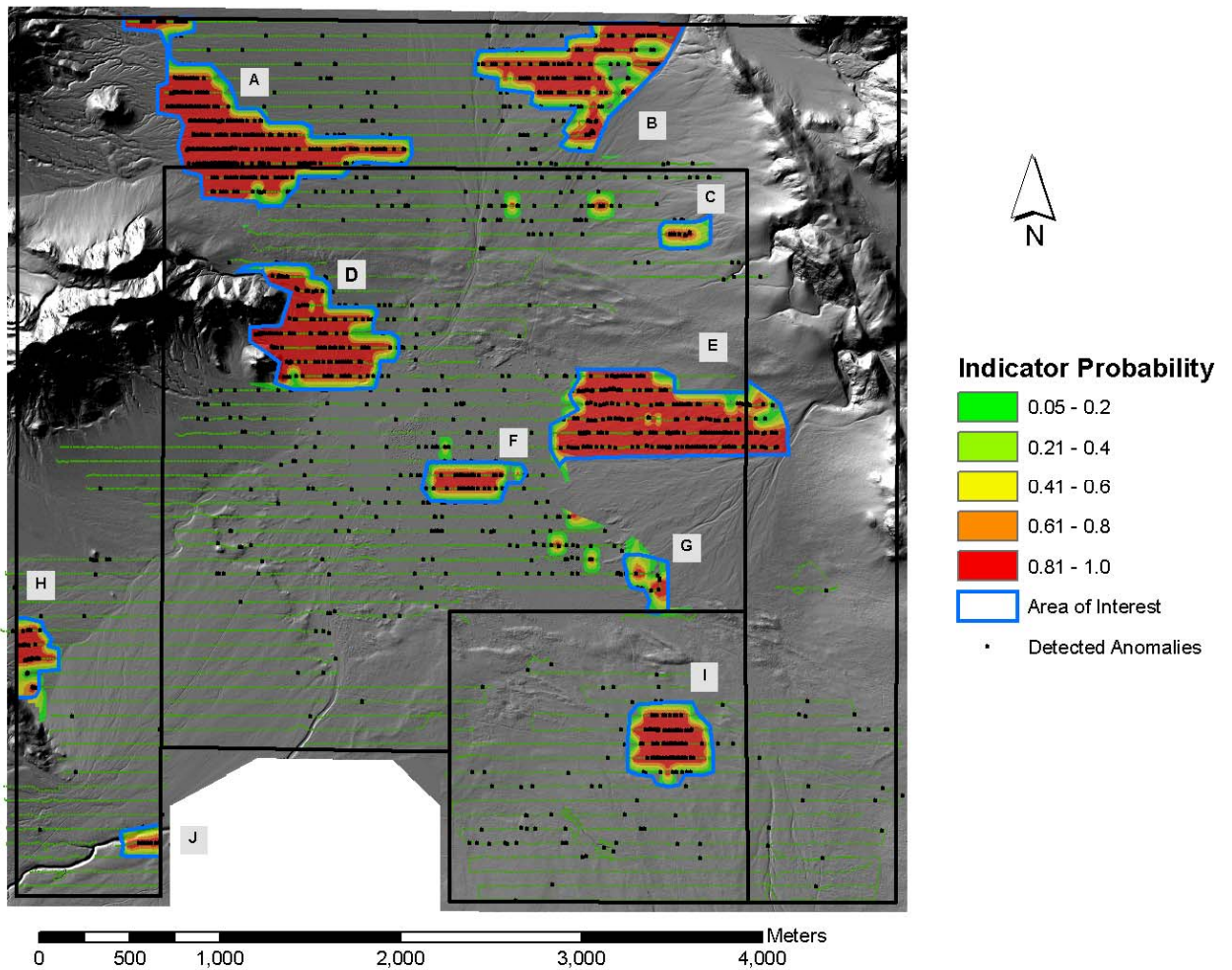


**Figure 14.** Indicator kriging results and delimited AOIs developed using anomaly data from the conservative transect design.

18

As part of the kriging process, it was necessary to model the spatial variability of the anomaly density data. This spatial variability was represented using semivariograms of the anomaly density data. Semivariograms model how the variance between data points changes as the spatial distance between any two points increases. Typically the variance increases as the distance between points increases. Figure 15 presents the indicator semivariogram developed using the transect data from the conservative design. The points in this figure represent the variance values computed at specific lag distances. The solid line represents the analytic model fit to the data points. This analytical model is used during the kriging procedures. The parameters describing these curves for all of the semivariogram models used in analysis of the Victorville transect data are provided in Appendix A.
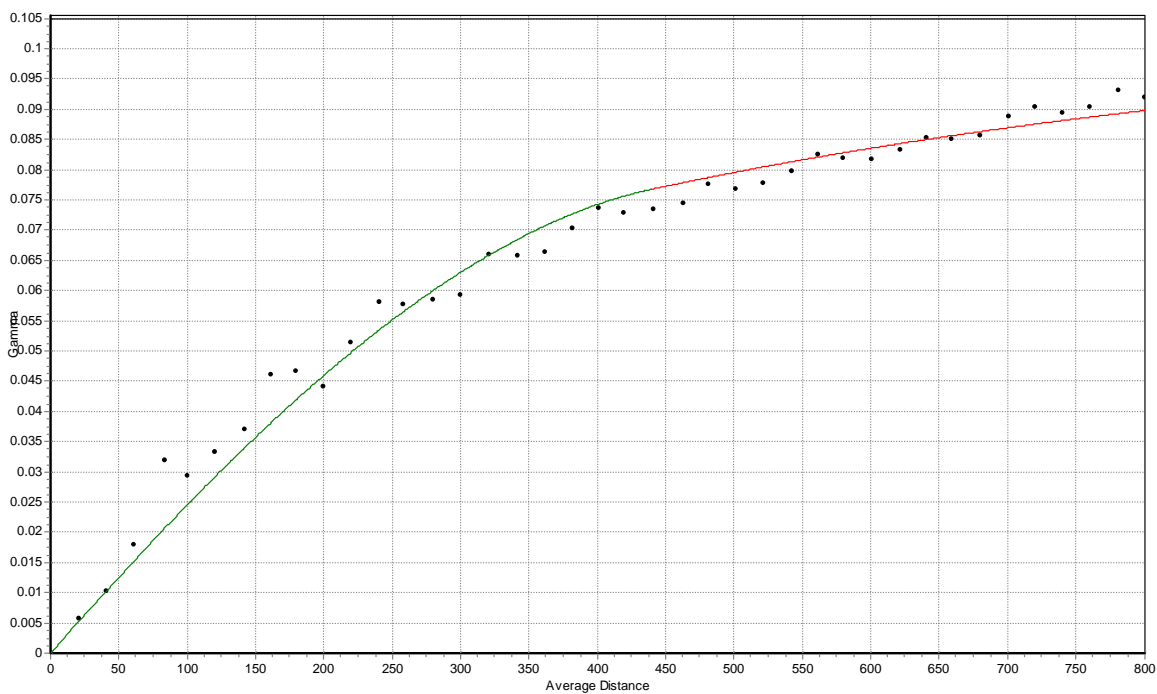


**Figure 15.** Semivariogram model and observational data for conservative transect design IK analysis. Units of X-axis are in meters.

The 10 AOI boundaries shown in Figure 14 and their letter designations correspond to the flagged high-density areas depicted in Figure 12. Some of the largest AOIs (A, B, D, and E) are located along the margins of the alluvial basin on the flanks of the adjacent slopes. These AOIs also contain some of the highest anomaly densities measured at the Victorville site. The complete extent of these high-density areas is not fully delineated and likely extends beyond the limits of the sampling transects. The configuration and location of these high-density areas suggests that they are not range-related features and instead represent local geologic noise. This issue is investigated further in Section 4.7. Of the remaining AOIs (C, F, G, H, I, and J), only two (F and I) have their margins fully defined through density contrast across fully-crossing sample transects. In addition, AOIs F and I are the only areas of interest along the central axis of the basin. All the

other AOIs are near the margins of the basin and are not fully defined by density contrast from crossing transects.

Ordinary Kriging was used to develop continuous anomaly density maps for the entire Victorville WAA site using anomaly data from the conservative transect design. The kriging estimates were computed using 20-by-20-m grid cells using the smoothed anomaly density values. The averaging window was 300-by-100 m and oriented with its long axis in the east-west direction. A semivariogram model specific to this data set was developed for use in the OK. The parameters for this semivariogram model are listed in Appendix A.

Figure 16 presents a map of the anomaly densities (i.e., ApA) estimated from the OK analysis. The color-filled contours indicate anomaly densities; areas without a color overlay have estimated densities below 20 ApA. As shown in this figure, the identified AOIs enclose the highest anomaly density locations and correspond with the IK results presented above.
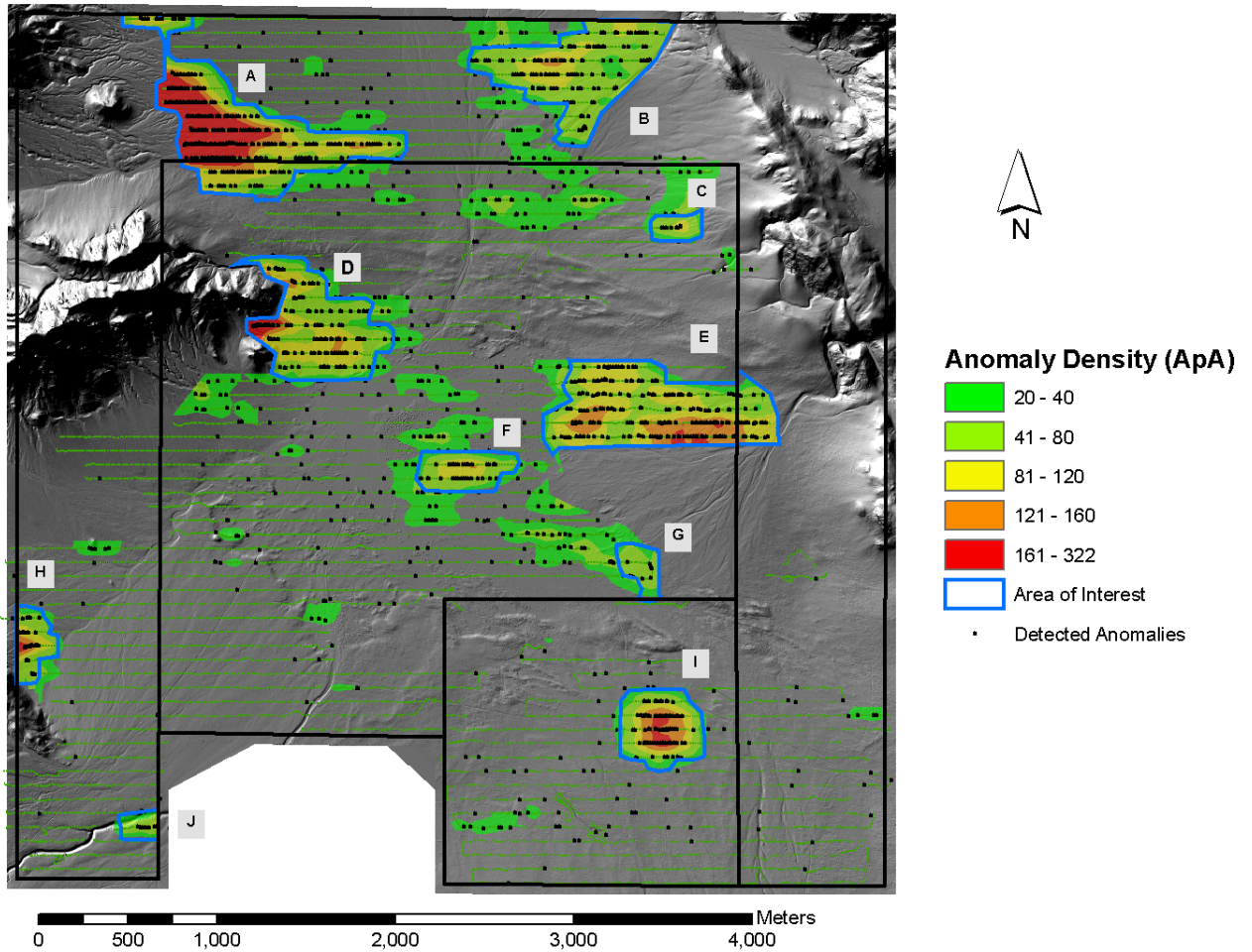


**Figure 16.** Anomaly density map of the Victorville conservative design based on kriging results. The AOI boundaries shown in light blue correspond to those developed using IK as shown in Figure 14.

### 4.3. Victorville Conservative with Additional Transect Design

Analyses of additional transects within the study were requested based on the initial analysis of the full transect design data to better delineate and identify suspected target areas and potential high-density areas. Each additional transect request (ATR) was designed to have transect coverage in the middle of the suspect target areas to improve density estimates used to identify areas of high density. Also, each ATR had transect coverage along the edges of the suspect target areas to improve perimeter delineation as well as density estimation. Typically 3 or 4 evenly spaced transects are requested to cover the identified potential target areas. The three additional transect requests on or near the bed of Means Dry Lake (ATR-3, ATR-4, and TC-03) were based on the identified high-density areas and previous information from the ASR of target areas lying within the lake bed, while ATR-1, ATR-2, and ATR-5 were requested to verify isolated and relatively small high-density areas. These additional transects were requested while the geophysical survey team was onsite completing the initially requested work. Figure 17 shows the full transect design with the additional requested transects (blue lines). The effects of these additional transect requests on the final results are detailed in Section 4.4.

#### 4.3.1. Additional Transect Requests around Means Dry Lake Bed

The transects requested in TC-03 lie in an identified cratered area on the bed of Means Dry Lake. However, the initial transects gathered in this cratered area did not show a high anomaly count, and additional transects were requested to validate the density estimates in this area. ATR-3, a relatively small and potentially isolated area with a high anomaly density based on the initial transect design, was located at the tip of the bed of Means Dry Lake. The additional transects were requested to improve survey coverage and anomaly density estimates. The area contained in ATR-4 had a high anomaly density but did not encompass the identified cratered area in this location. Thus, the additional transects were requested to improve boundary delineation of this area.

#### 4.3.2. Additional Transect Requests to Verify Isolated High-Density Areas

The identified high-density areas contained in ATR-1, 2, and 5 were small isolated areas that did not fall in or around areas with any other potential target area evidence. The additional transects were requested to improve survey coverage, which improves the ability to distinguish between background and target area densities and improves the precision of the density estimates for these smaller areas.
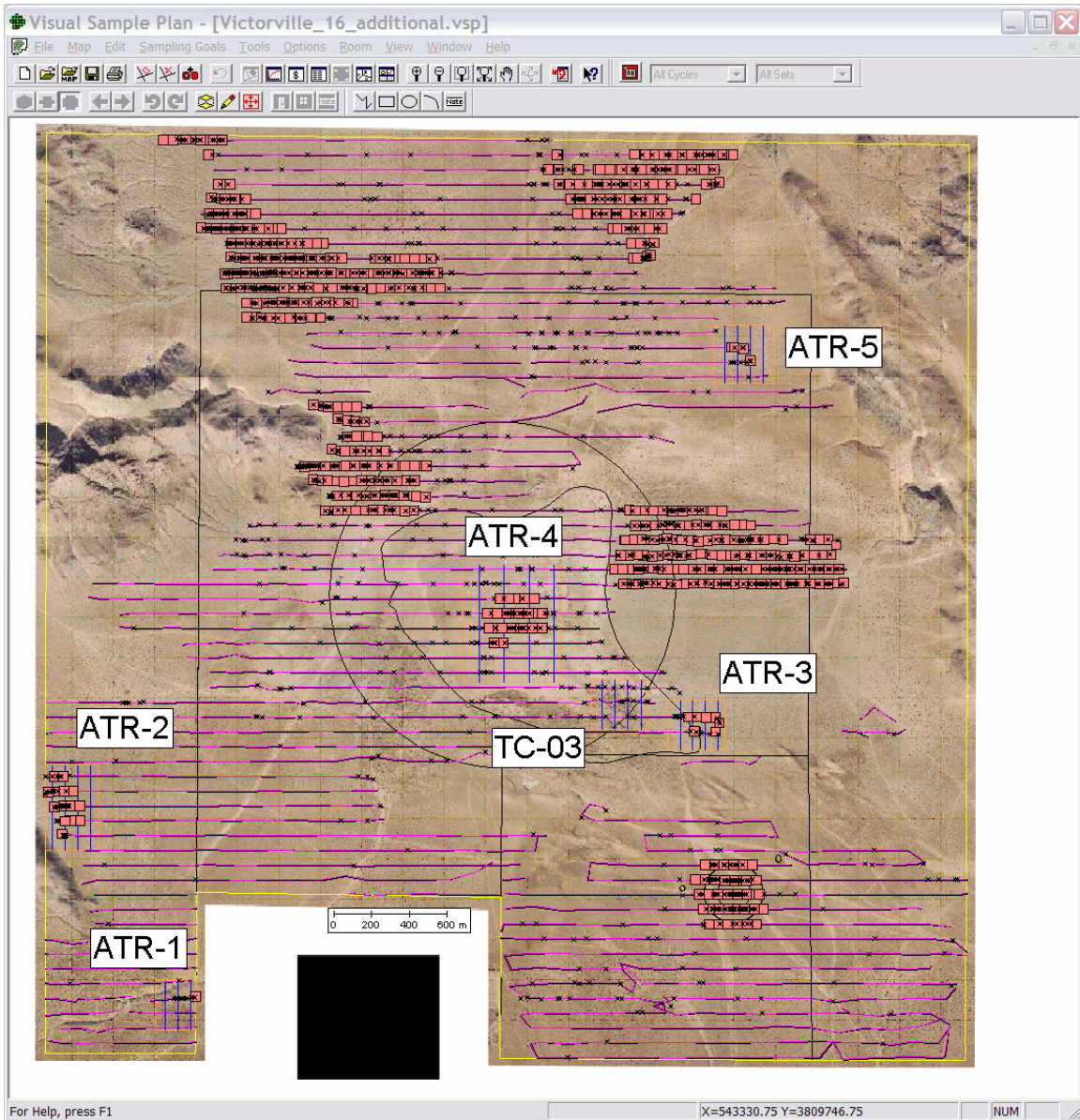
**Figure 17.** Additional transect requests (blue lines) based on potential high-density areas depicted by red boxes (flagged areas) with the transect and anomaly data for the conservative survey.

## 4.4.   Victorville Conservative with Additional Transect Design Analysis

The actual course traversed by the geophysical survey team is depicted in Figure 18. This figure shows the additional north-south transects that were requested to better delineate high-density areas.  Similar to Figure 11, the orange shaded areas in Figure 18 represent generally inaccessible regions.  The terrain in the TC-03 area limited the retrieval of data obtained by the survey team.  Of the four transects requested in this area, only a portion of one transect was collected.  Because of its limited use, it was not included in the analysis.  Within the 3467 accessible acres (yellow area), the additional surveyed transects increased the coverage to approximately 89 acres (2.55 percent coverage).
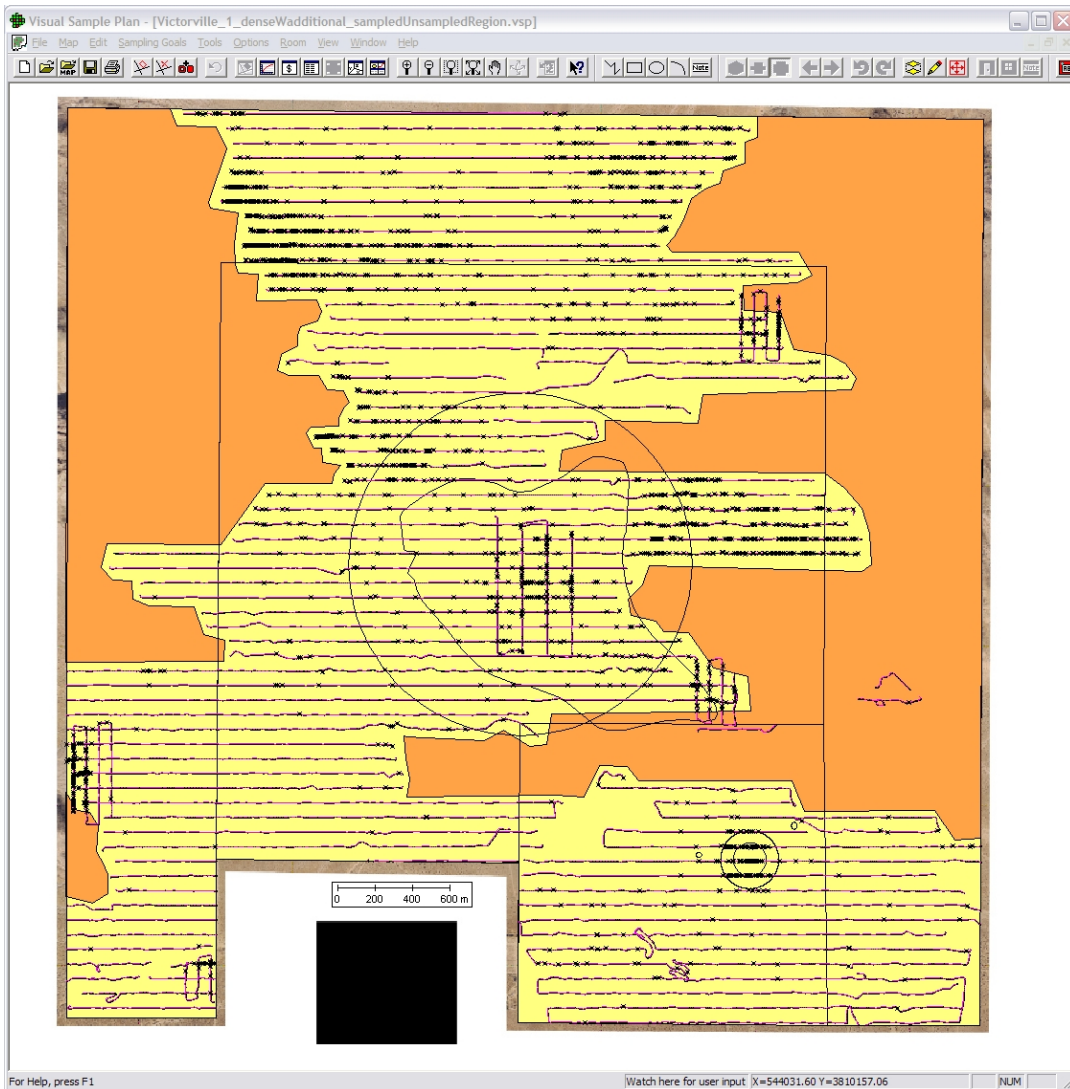
**Figure 18.** Depiction of the actual transects gathered based on the conservative transect design with additional transect requests. The black dots represent identified anomalies.

### 4.4.1.  Target Area Identification, Delineation, and Density Estimation

Figure 19 shows the flagged areas of high density based on a 300-m-diameter window and a critical density of 53 ApA for the conservative design with additional transects. The AOIs originally identified from the conservative design are again labeled A through J (Areas F, G, and I correspond to target areas identified in the CSM). The additional transects requested in Area J show that this area is no longer flagged as a high-density area. The portion of Area J that had multiple anomalies adjacently located was confirmed by survey team to contain camping debris. All other areas where additional transects were requested continue to be identified as high-density areas. Although Area J is no longer a high-density area, the identifier will be maintained for discussion purposes.

23
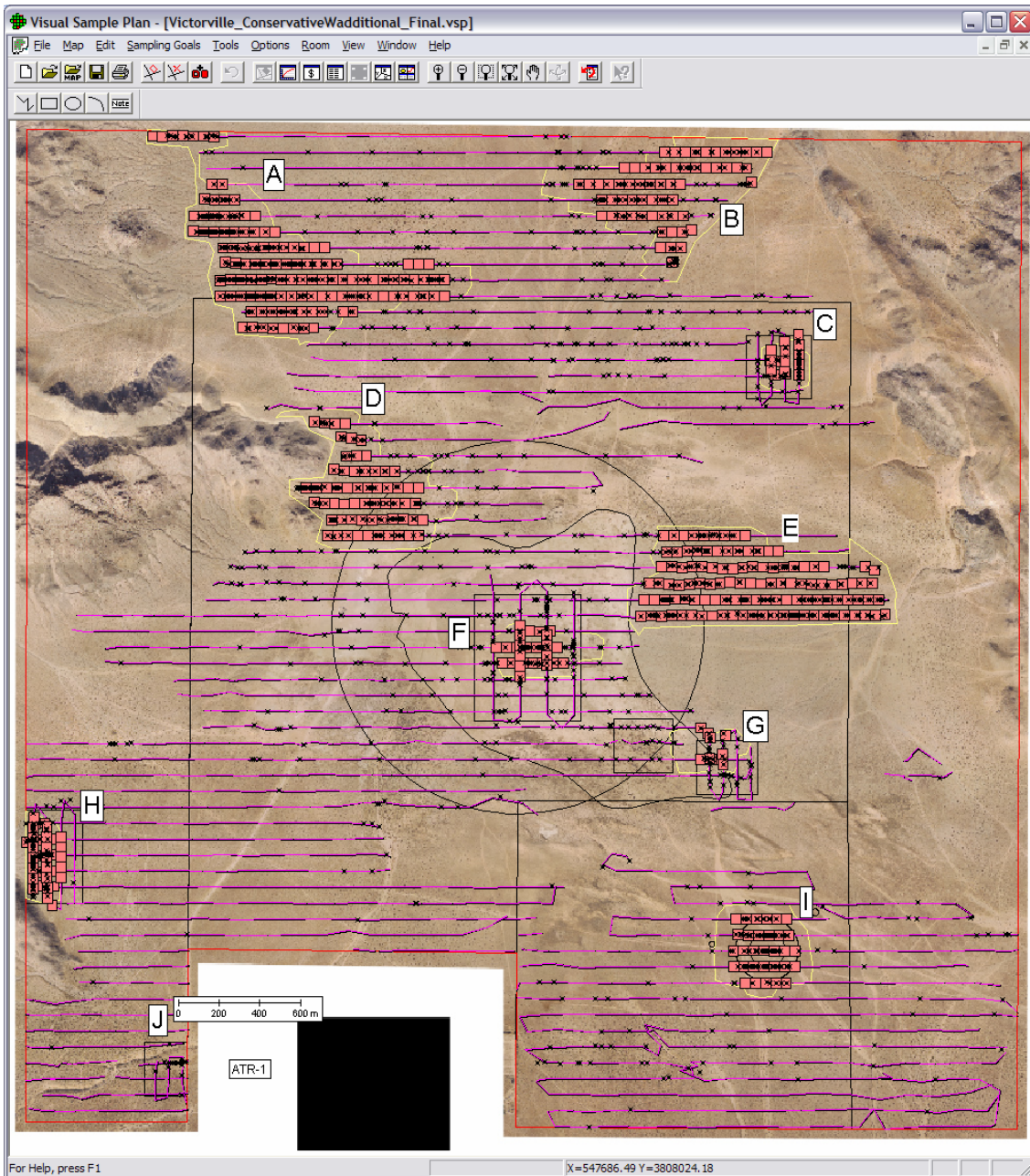
**Figure 19.** Flagged high-density AOIs for the conservative transect design with additional transects based on a 300-m-diameter window and a critical density of 53 ApA. All identified areas of high density remained except for Area J. The survey team mentioned that this area did contain camping debris. High-density-area delineations are depicted with yellow lines.

Figure 20 shows the IK probability levels for the conservative transect design with added north-south transects using an IK threshold of 53 ApA. Areas with a probability of 0.05 or greater of being above the 53 ApA threshold are indicated by color-filled probability contours. These areas were included as part of the information used in determining the final boundaries for the AOIs.

The semivariogram for the conservative plus additional transects data set was examined, and a new semivariogram analytical model developed. This new model differed only slightly from that developed for the original conservative design transects. The parameters for the new analytical model are listed in Appendix A.

The additional transects revealed that Area-J has a much lower anomaly density than estimated using the original conservative transect design. Subsequently Area-J was eliminated as an AOI. The remaining nine AOIs are centered at the same locations as those originally identified in the conservative transect design. Areas of interest where additional transects were added had their boundaries refined from the additional information; AOIs for which additional transects were not collected have the same boundaries as shown in the conservative transect design. As before, some of the largest AOIs (A, B, D, and E) are located along the margins of the alluvial basin along the flanks of the adjacent slopes. Only AOIs F and I have margin definitions from fully crossing transects.
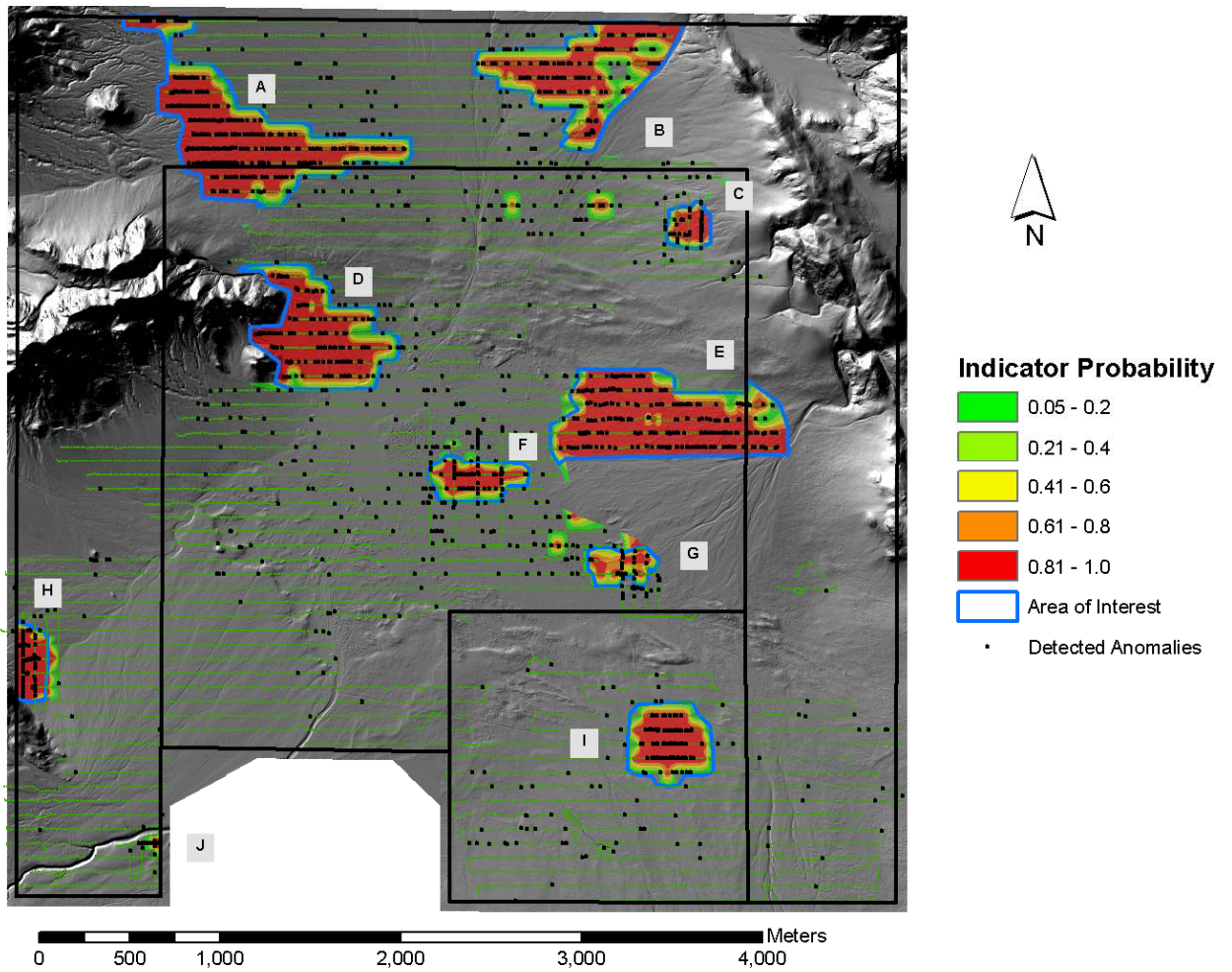


**Figure 20.** Indicator Kriging results and delimited AOIs developed using anomaly data from the conservative transect design with additional north-south transects.

25

Figure 21 shows kriged estimates of anomaly density developed from the conservative transect design with additional transects. This estimate was developed using all anomaly data from transect-based, average anomaly concentrations. The averaging window was 300 m by 100 m and oriented with its long axis in the east-west direction. As in the previously presented density estimates, these estimates were developed with OK using a 20-by-20-m grid cell. A semivariogram model specific to this data set was developed for use in the OK. The parameters for the semivariogram model are listed in Appendix A. The color-filled contours in Figure 21 indicate anomaly densities; areas without a color overlay have estimated densities below 20 ApA. As shown in this figure, the identified AOIs enclose the highest anomaly density locations and correspond to the IK results presented above.
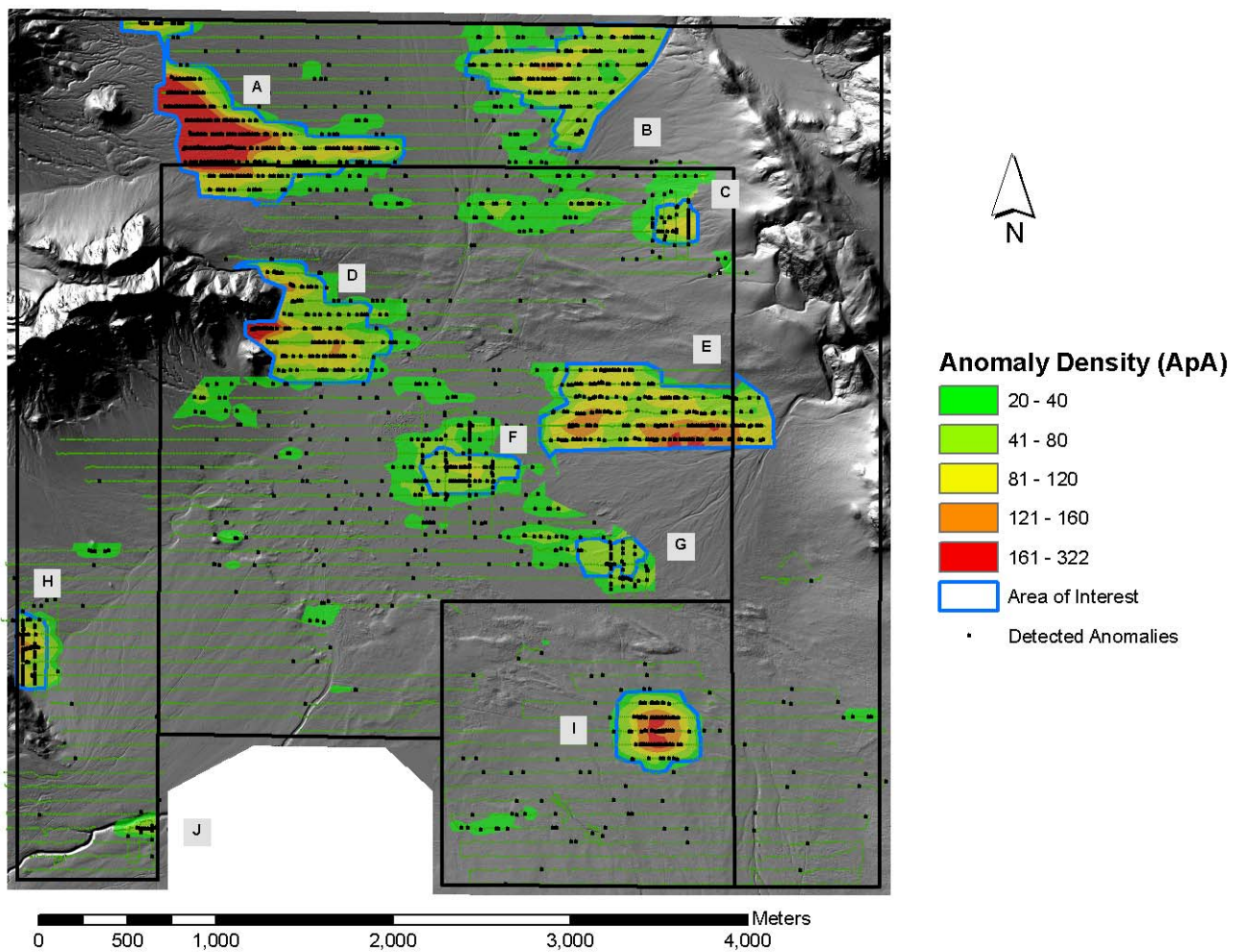


**Figure 21.** Density map of the Victorville conservative design with additional transects based on kriging results. The AOI boundaries shown in light blue correspond to those developed using IK as shown in Figure 20.

## 4.5.    Victorville Sparse Transect Design

The sparse transect design was based on the high-altitude, precision-practice-bomb target (VV-15) located on the southeastern portion of the site.  Based on available imagery of the VV-15 area, the visible target circles are 180 m in diameter.  As described in section 4.1, this precision bombing target appears to have similarities to those found on the Pueblo Precision Bombing Range located in southern Colorado (Figure 9).  Given these similarities, a transect design that has a 100 percent probability of traversing a 500-ft (153-m) diameter circular target area was desired.  This transect design request (shown in Figure 23) covered 1.29 percent of the study area with 2-m-wide transects spaced 154.4 m apart on centers.  This design had a good probability of detection, as shown in Figure 22, with only half of the transects required (i.e., less coverage) as compared to the final design referenced in Section 4.1.  This sparse transect design is a subset of the conservative design and it was created to compare the extent that less transect data could achieve the same conclusions of the conservative transect design.
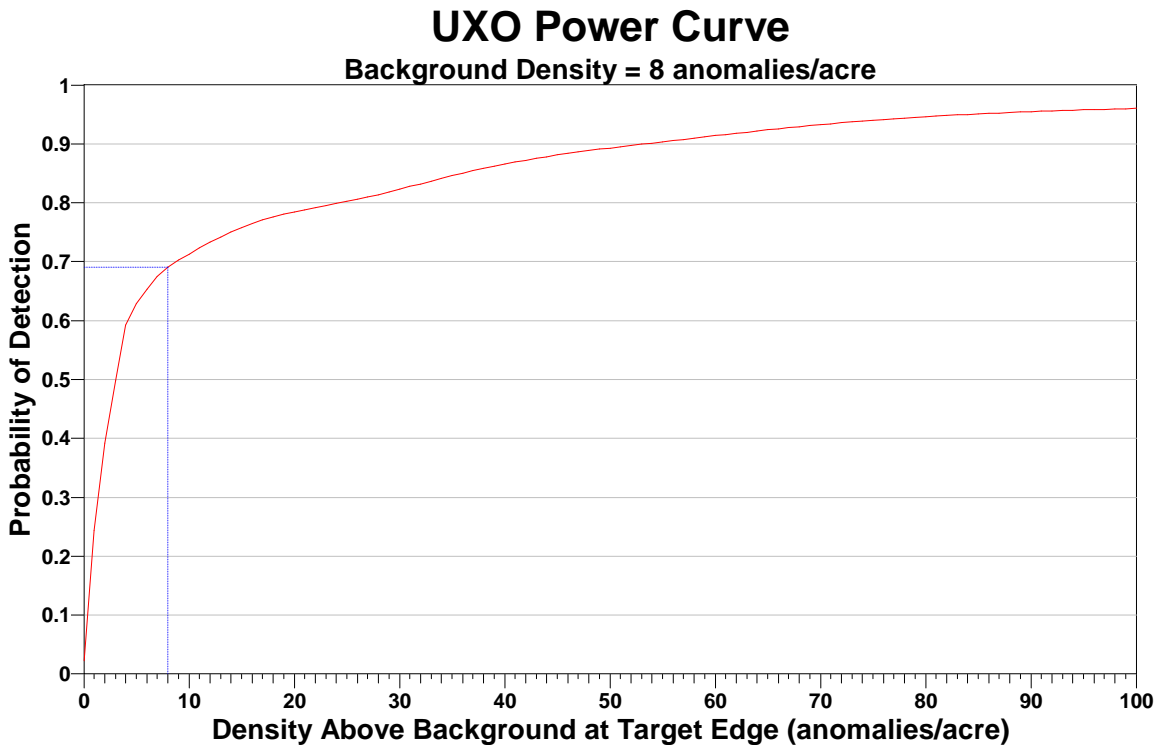


**Figure 22.**  Power curve to identify a 500-ft (153-m) diameter circular target area with 2-m-wide transects spaced 154.4 m apart on centers.  Note that the density above background axis has a much larger range than Figure 10.
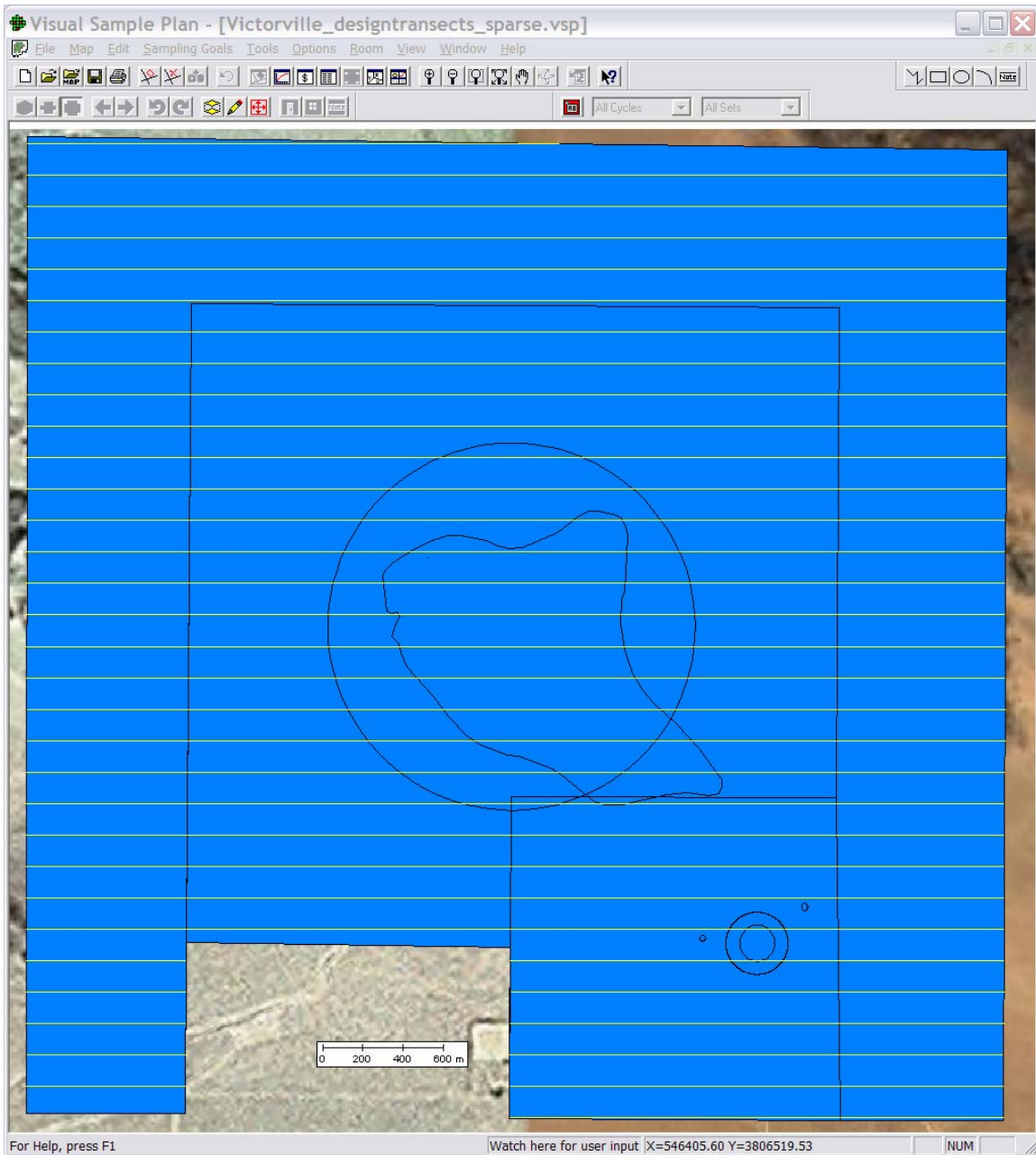
**Figure 23.** Sparse transect design based on the odd transects from the conservative transect design described above.

## 4.6.   Victorville Sparse Transect Design Analysis

The actual course traversed by the geophysical survey team based on the sparse transect design is depicted in Figure 24 where the orange regions represent areas generally inaccessible to the towed array system.  Within the 3467 accessible acres (yellow area), the coverage based on the sparse design was approximately 43 acres (1.24 percent coverage).  The coverage of 1.24 percent is roughly one-half of the actual coverage obtained in the original conservative design.
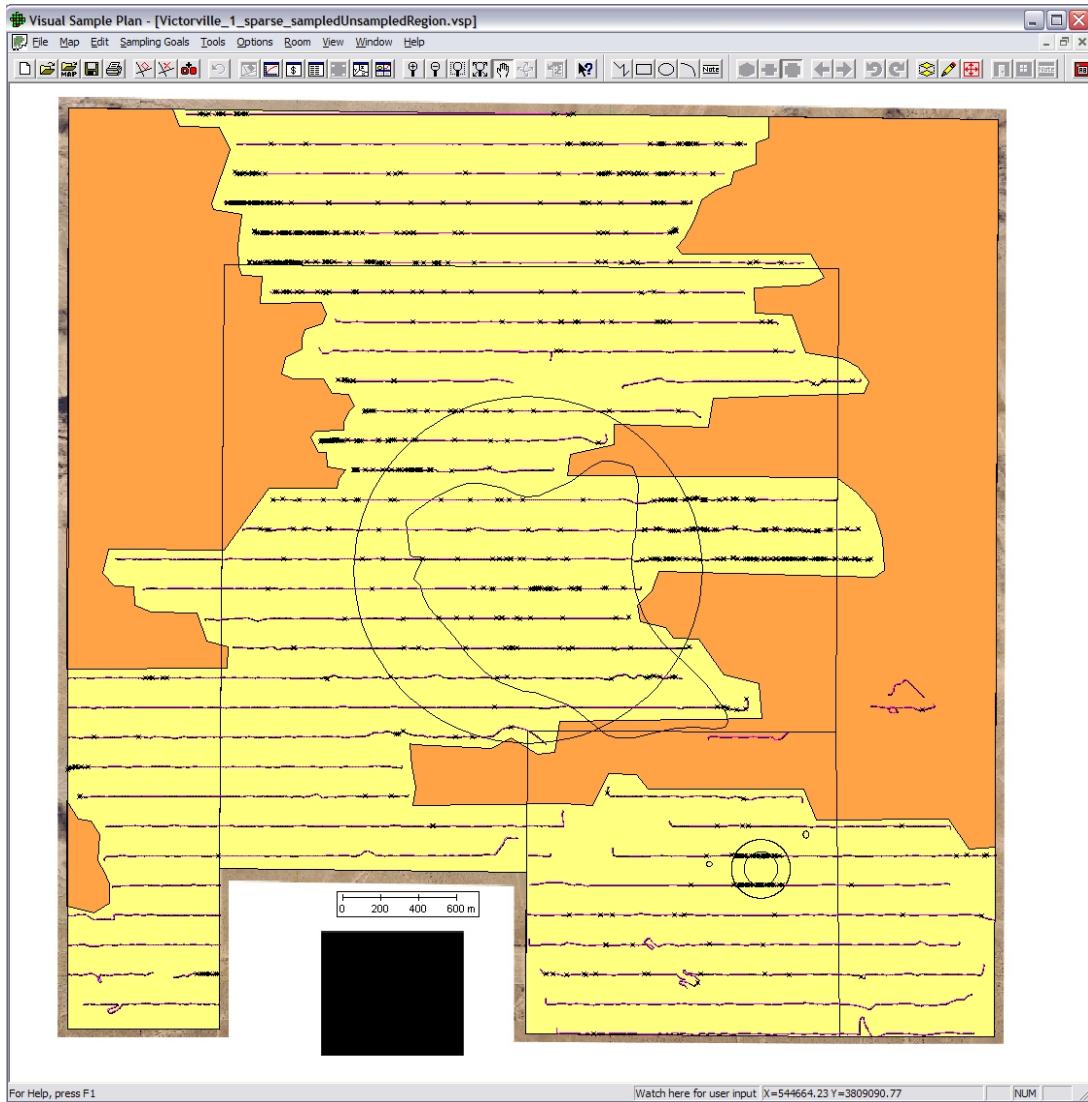
**Figure 24.** Depiction of the actual transects gathered based on the sparse transect design. The orange and yellow areas identify the separation between generally accessible and inaccessible areas**.**

### 4.6.1. Target Area Identification, Delineation, and Density Estimation

Figure 26 shows the flagged areas of high density based on a 300-m-diameter window and a critical density of 53 ApA. This critical density was selected based on the description in Section 3 using the histogram shown in Figure 25. The AOIs from the conservative design are labeled A through J. Areas G and H were flagged as high-density areas, but the number of the respective flags in these areas were less when compared to the conservative design. Based on the sparse transect design, Area C was not identified as a high-density area. Area J, which was eliminated as a high-density area in the previous analysis (conservative design with additional transects), appears as a high-density area in the sparse transect design.
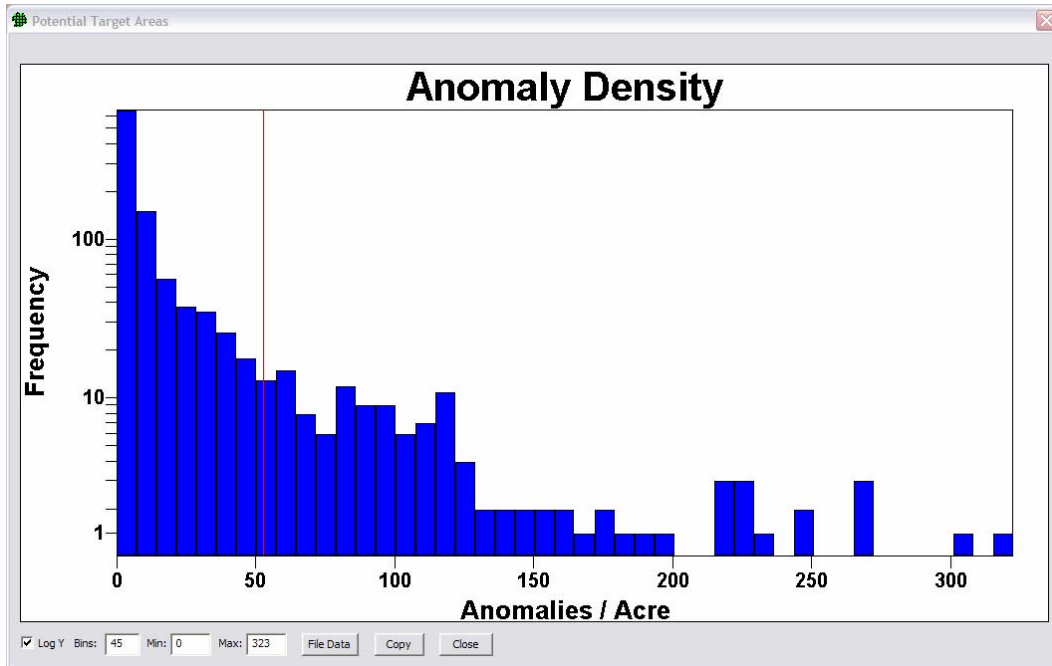
**Figure 25.** Histogram of 300-m-diameter window densities for the surveyed transects from the sparse transect design.

Figure 27 shows the IK probability levels for the sparse transect design using an IK threshold of 53 ApA. Areas with a probability of 0.05 or greater of being above the 53 ApA threshold are indicated by color-filled probability contours. These areas were included as part of the information used in determining the final boundaries for the AOIs.

A new semivariogram analytical model was developed for the sparse transect design data set. The parameters for this model are listed in Appendix A.

The IK results from the sparse transect design are comparable to those from the conservative transect design. The locations and general shapes of the AOI boundaries are very similar. The primary difference in the results from the sparse design is the absence of an identified high-density area in the region identified as Area C. In this case, the adjacent transects (not included here) that were part of the conservative design provided additional information that highlighted this area as high density in the conservative design.
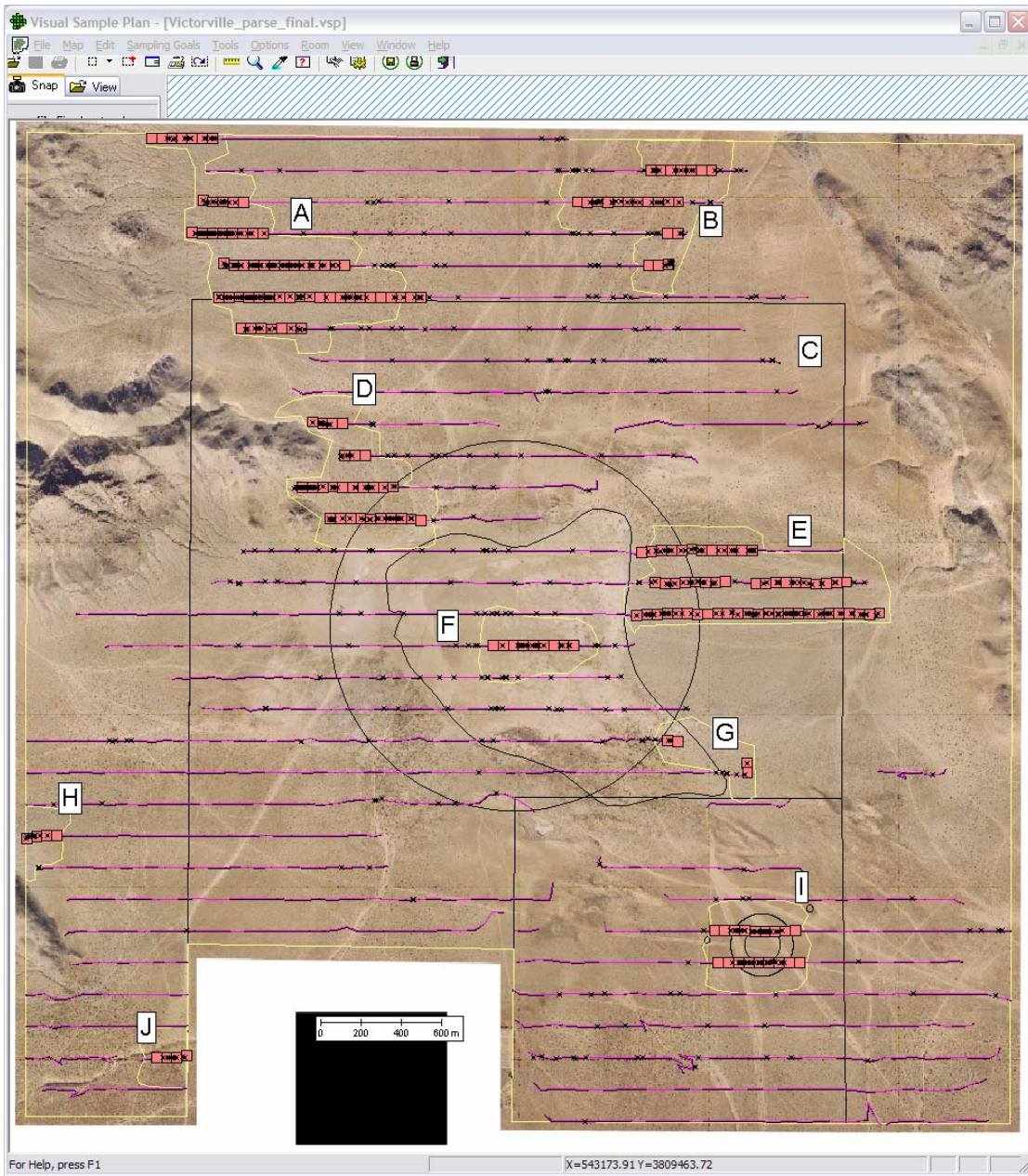
**Figure 26.** Flagged high-density AOIs for the sparse transect design based on a 300-m-diameter window and a critical density of 53 ApA. High-density-area delineations are depicted with yellow lines.
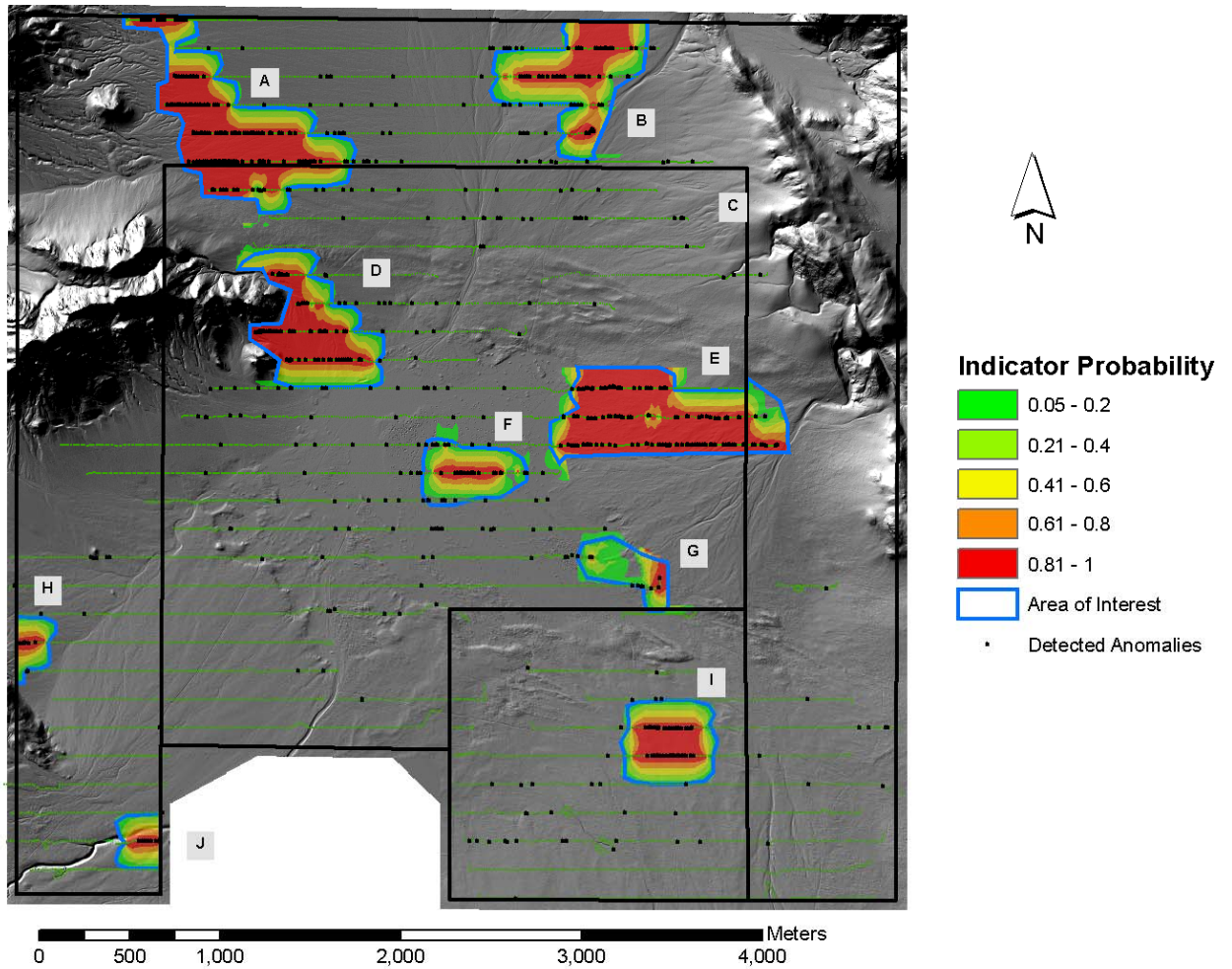
**Figure 27.** Indicator Kriging results and delimited AOIs developed using anomaly data from the sparse transect design.

Figure 28 shows kriged estimates of anomaly density developed from the sparse transect design. This analysis was developed using all anomaly data from sparse transect-based, average anomaly concentrations. The averaging window was 300 m by 100 m and oriented with its long axis in the east-west direction. As in the previously presented density estimates these estimates were developed with OK using a 20-by-20-m grid cell. A semivariogram model specific to this data set was developed for use in the OK. The parameters for this model are listed in Appendix A. The initial segment of the sparse transect design semivariogram had a slightly lower sill and longer range than that from the conservative design. The color-filled contours in Figure 28 indicate anomaly densities; areas without a color overlay have estimated densities below 20 APA. As shown in this figure, the identified AOIs enclose the highest anomaly density locations and correspond with the IK results presented above. Although Area C was not designated as an AOI for this scenario based on the VSP flagging routine and IK results, it does contain higher anomaly densities than the surrounding region as shown by the OK density kriging.
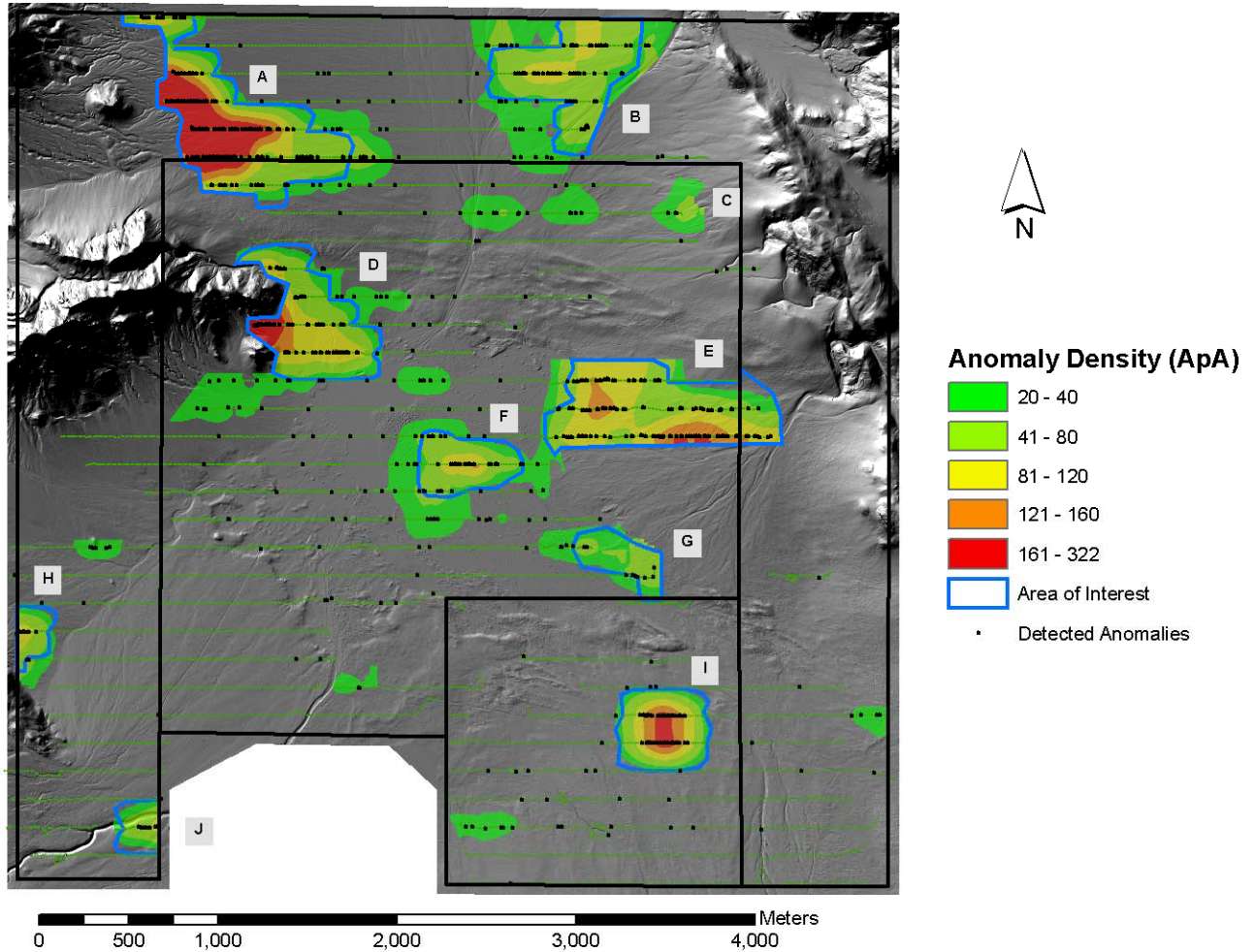
**Figure 28.** Anomaly density map based on sparse transect design. The light blue polygons correspond to the AOI boundaries defined by IK (Figure 27).

## 4.7. Victorville Geological Anomaly Filtered Data Analysis.

The Victorville Precision Bombing Range lies within a geologic setting with a large natural magnetic signature. Figure 29 shows a compilation of aeromagnetic data for southern California. As shown in this figure, there is a large magnetic anomaly located in the vicinity of the Victorville Precision Bombing Range. This suggests that local geologic materials have introduced noise into the geophysical transect data collected at the Victorville WAA Site. Geologic noise in the magnetic anomaly data also is evidenced by the density of magnetic anomalies seen on the alluvial slopes adjacent to the Victorville Precision Bombing Range. As seen in the transect data shown in previous figures, the greatest anomaly densities occur on the alluvial slopes that connect the bedrock ridges to the valley floor. In addition, in these areas, there is a general decrease in anomaly density with increasing distance from the bedrock ridges (Figure 21). These high-density areas also were noted in the field report submitted by the geophysical transect sampling team (Nova Research 2006). Reconnaissance of these areas by the geophysical field team revealed the terrain surface was covered with boulder to pebble

sized rock fragments. The field team hypothesized that these fragments may be the cause of the high anomaly counts in these areas. These complementary forms of evidence indicate that the anomaly transect data for the Victorville PBR likely contains some significant level of geologic noise and that some level of filtering of the anomaly data is worth investigation.
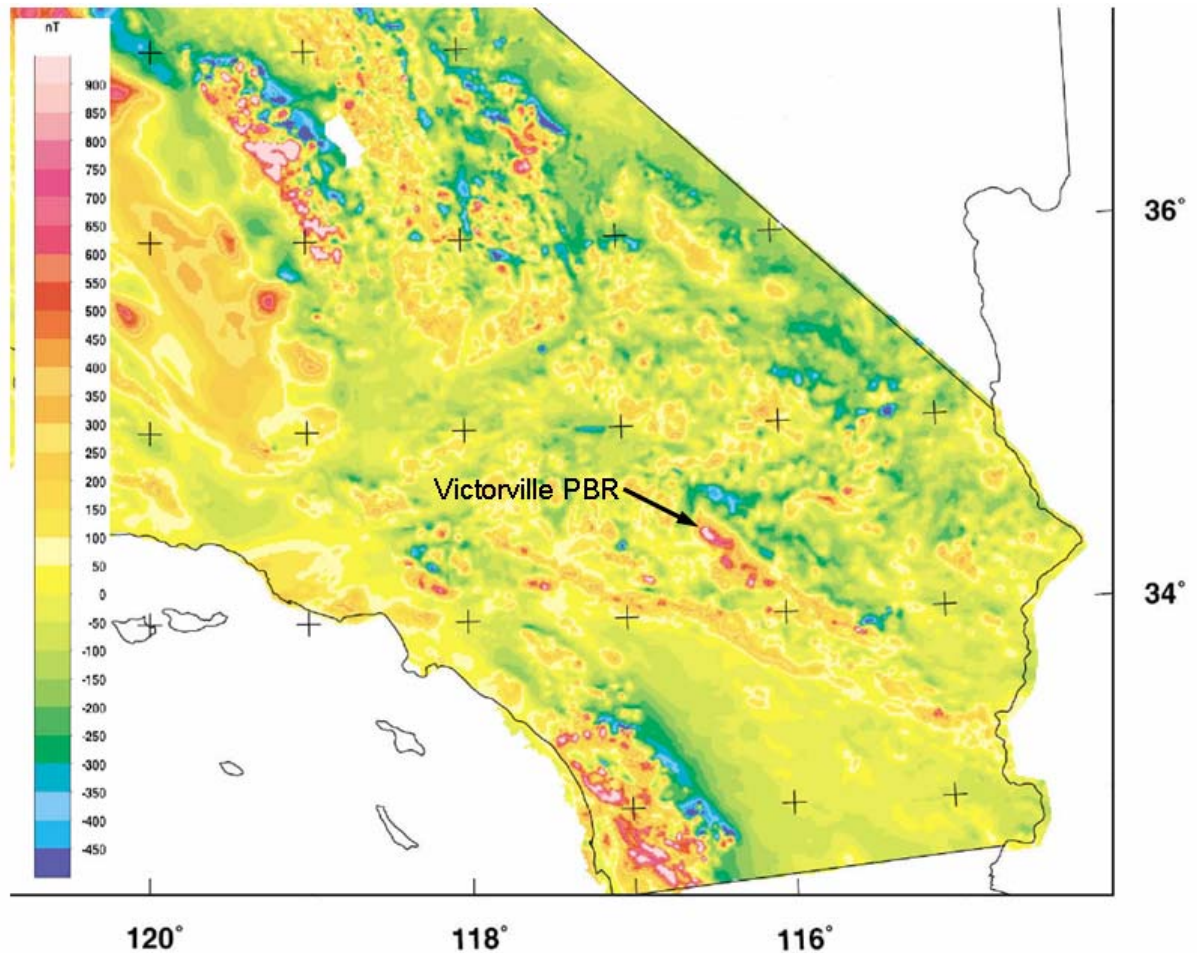


**Figure 29.** Small-scale magnetic anomaly map for Southern California after Roberts and Jachens (1999). The color scale is in nano-teslas and the location of Victorville Precision Bombing Range is shown by the arrow.

## 4.7.1. Geologic Anomaly Filtering Process

Because the Victorville range contains alluvial rock material capable of generating magnetic anomalies and based on this knowledge and the known history of the site, it would be reasonable to assume that the magnetic anomalies detected in the geophysical surveys originate from three different sources: 1) local rock debris (geologic noise), 2) anthropogenic clutter not related to DoD range activities, and 3) munitions related UXO and fragments. Following this assumption, a K-means cluster analysis was performed on the anomaly data with the assumption that three distinct anomaly types were present. The magnetic anomaly data from the conservative design with additional transect data set was used for this analysis.

The K-means clustering procedure operates by assigning data observations to each of k groups or clusters. Points are assigned to the cluster with the smallest Euclidean distance between the point and the cluster's centroid. All distances are computed in multivariate space using standardized variable values. The data points for the initial group definitions are randomly determined and observations may change groups as the analysis proceeds (non-hierarchical). Centroid values are dynamically computed as group assignments change. The number of clusters is predetermined (three in this case) and each observation is assigned to a single cluster. The process results in each observation being grouped with others which are closest to it in multivariate space. More details on K-means clustering can be found in Davis (1986).

Three anomaly based variables were used for cluster designation. The first variable was the transect anomaly density. This variable was included because it gives an indication of general spatial distribution of the anomalies. The second variable was the analytic signal value reported for each anomaly value. This feature was included based on general patterns of analytic signal observed in the geophysical data, which indicated that this variable may be useful in discriminating between anomalies generated by naturally occurring and anthropogenic source materials. The third and final variable included in the K-means cluster analysis was the distance from each anomaly location to the nearest rock outcrop. This distance was computed using the geographic location of each anomaly and the outline of rock outcrops for the Victorville area as obtained from the Soil Survey Geographic (SSURGO) database (USDA 2006). The rationale for this variable is the expectation that the density and size of surficial rock material will be greatest near the outcrop, and will diminish with increasing distance away from the outcrop.

Figure 30 shows the distribution of the three anomaly groupings as classified by the K-means procedure. Figure 31 and Figure 32 show box-and-whisker plots for the three clusters for each of the three defining variables with corresponding statistics presented in Table 3. Assuming the three anomaly sources hypothesized above hold (i.e., geologic noise, general clutter, and munitions related), then the most appropriate label for Group 1 would be geologic noise. Groups 2 and 3 are not as distinct and likely represent some mixture of general clutter and munitions related anomalies.

As shown in Figure 31 and Table 3, the analytic signal value for Group 1 tends to be lower and have a smaller inter-quartile range compared to Groups 2 and 3. This might be expected for natural materials distributed and sorted via alluvial processes. The anomaly density for Group 1 also shows a decreasing density with increasing distance from the outcrop source supporting the association of Group 1 with local geologic materials (see Figure 28).
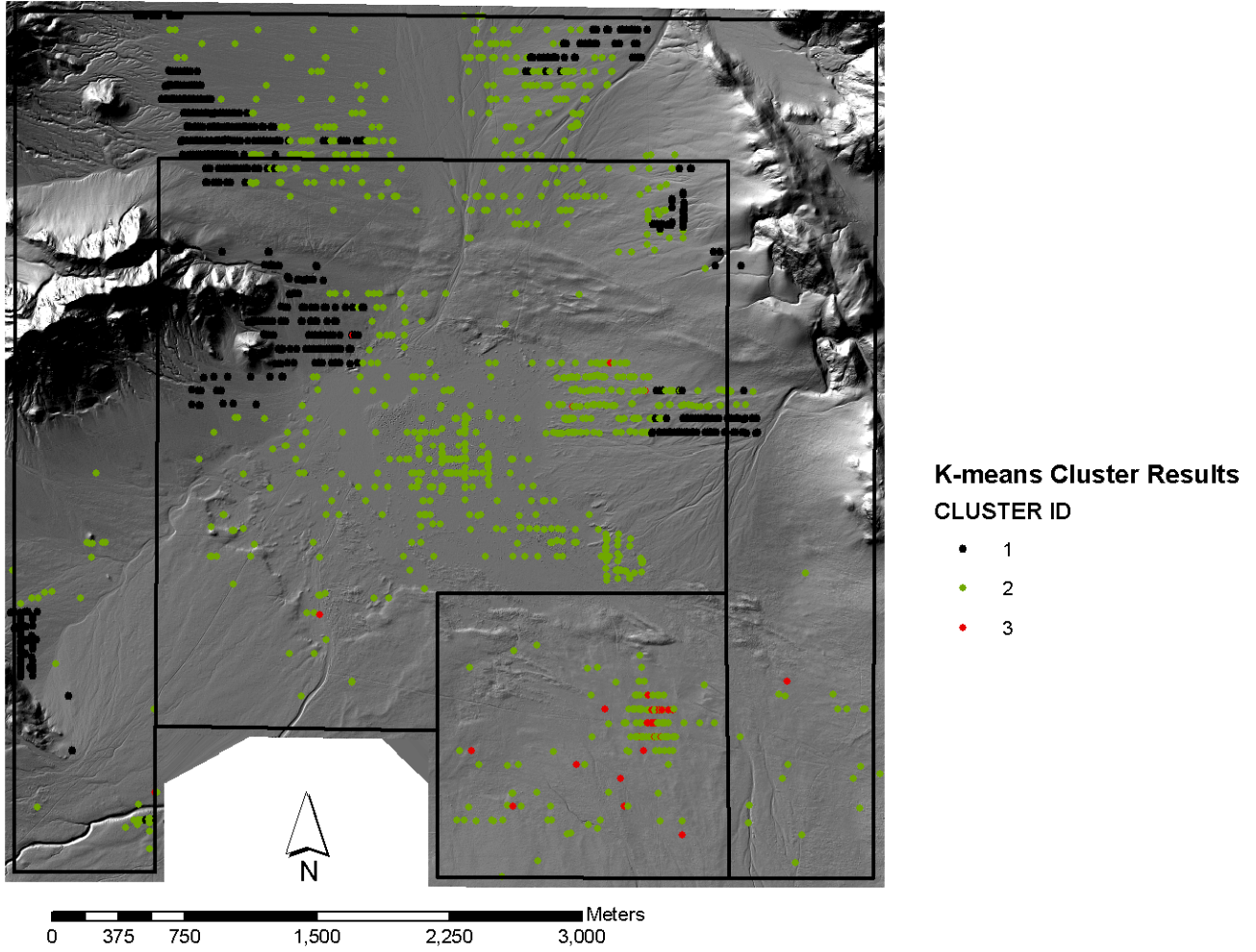
**Figure 30.** Spatial distribution of anomaly classifications based on K-means cluster analysis.
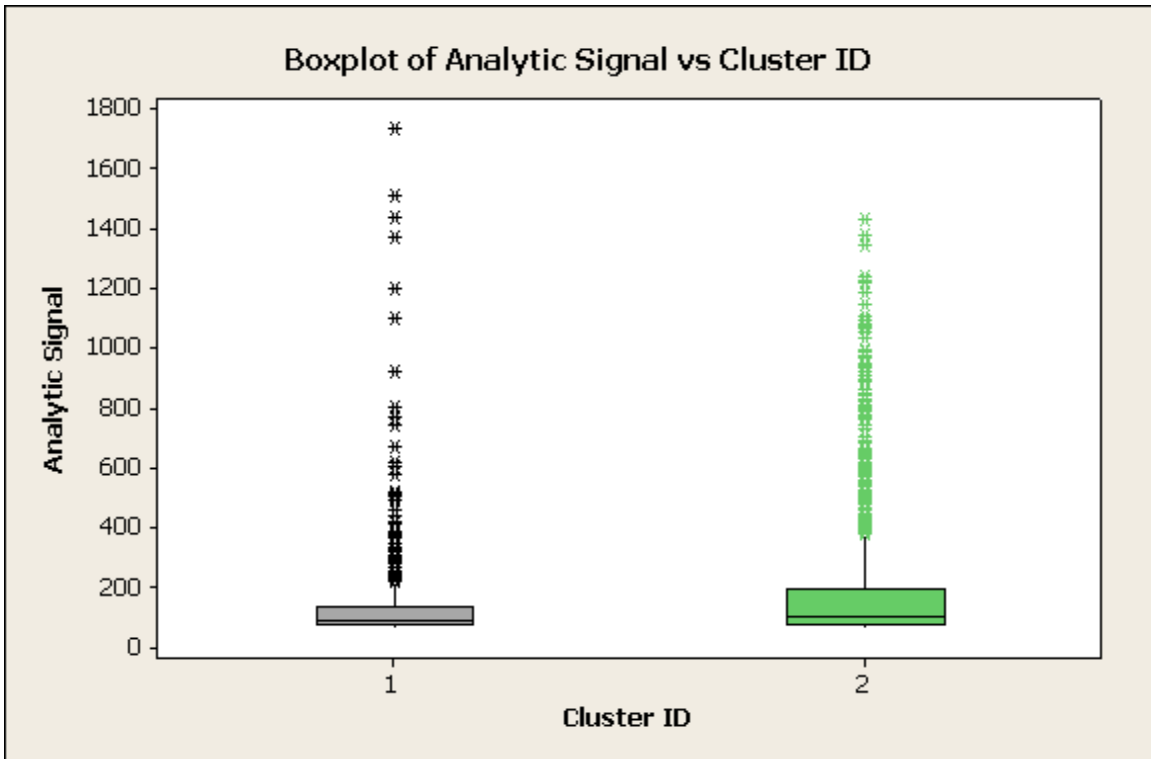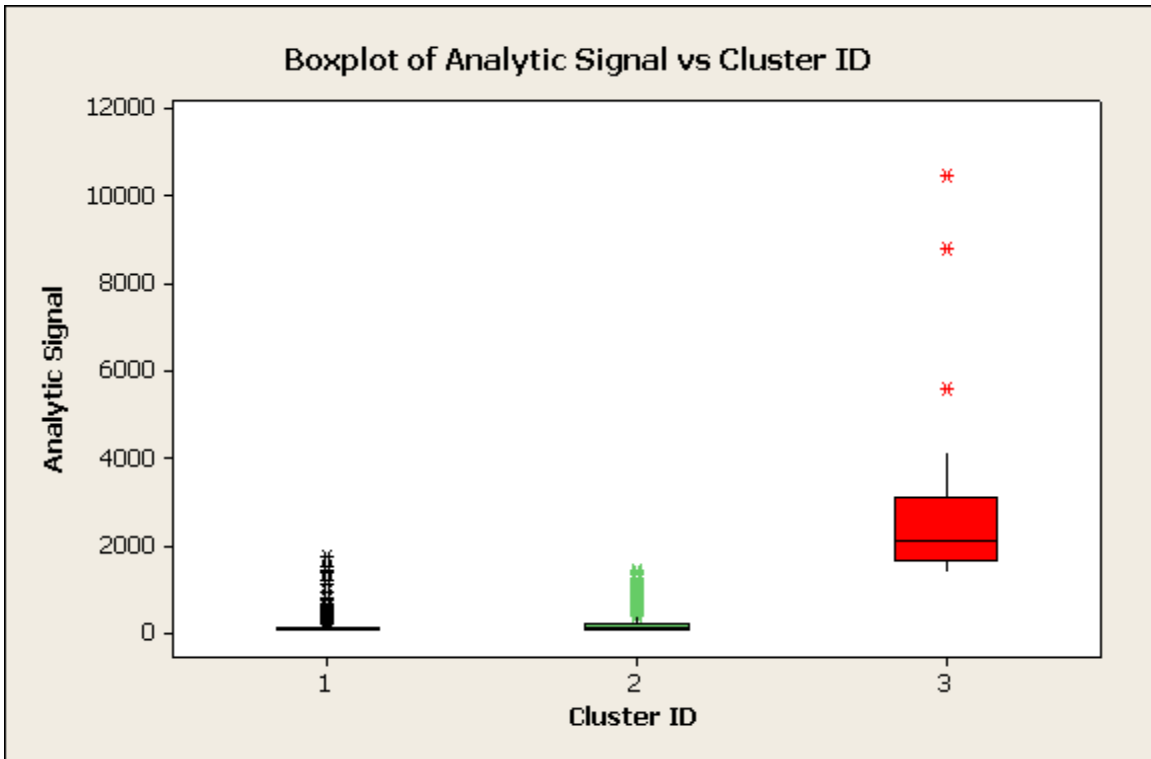
**Figure 31.** Box-and-whisker plots of analytic signal (nT/m) for each group resulting from the K-means cluster analysis. Top plot compares all three cluster groups; bottom plot compares only groups 1 and 2 and is rescaled to show details. The color scheme matches that used in Figure 30.
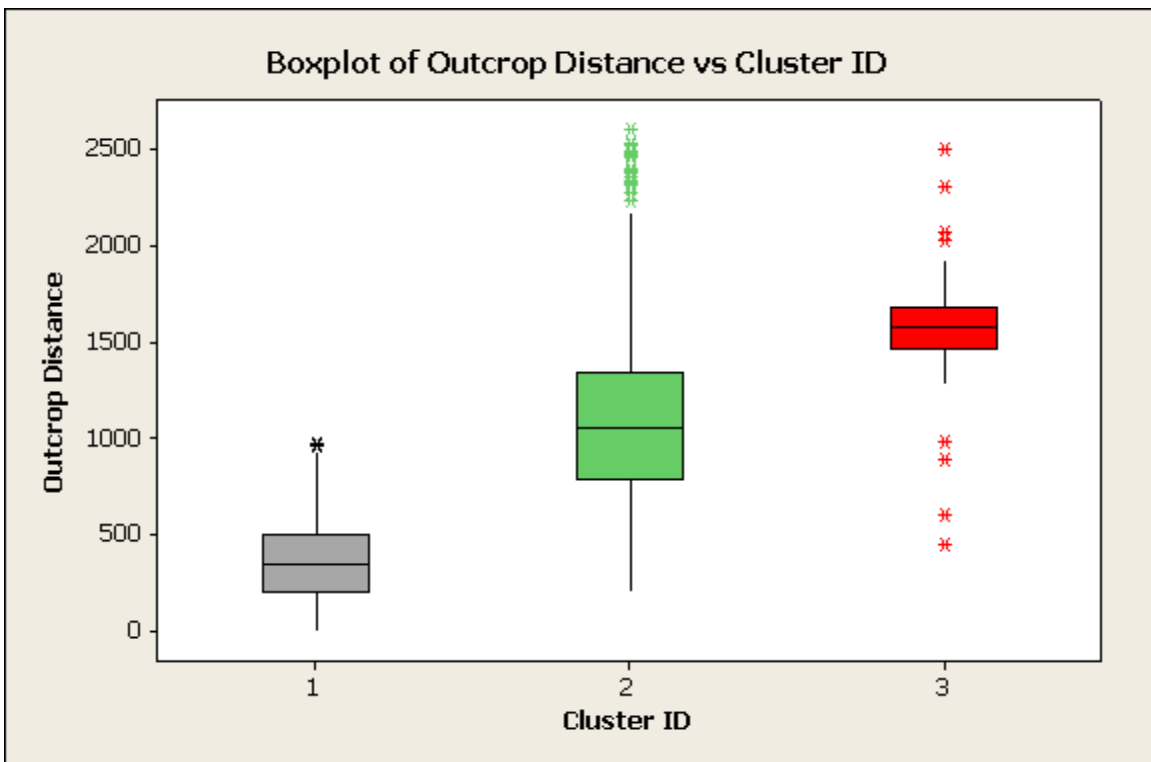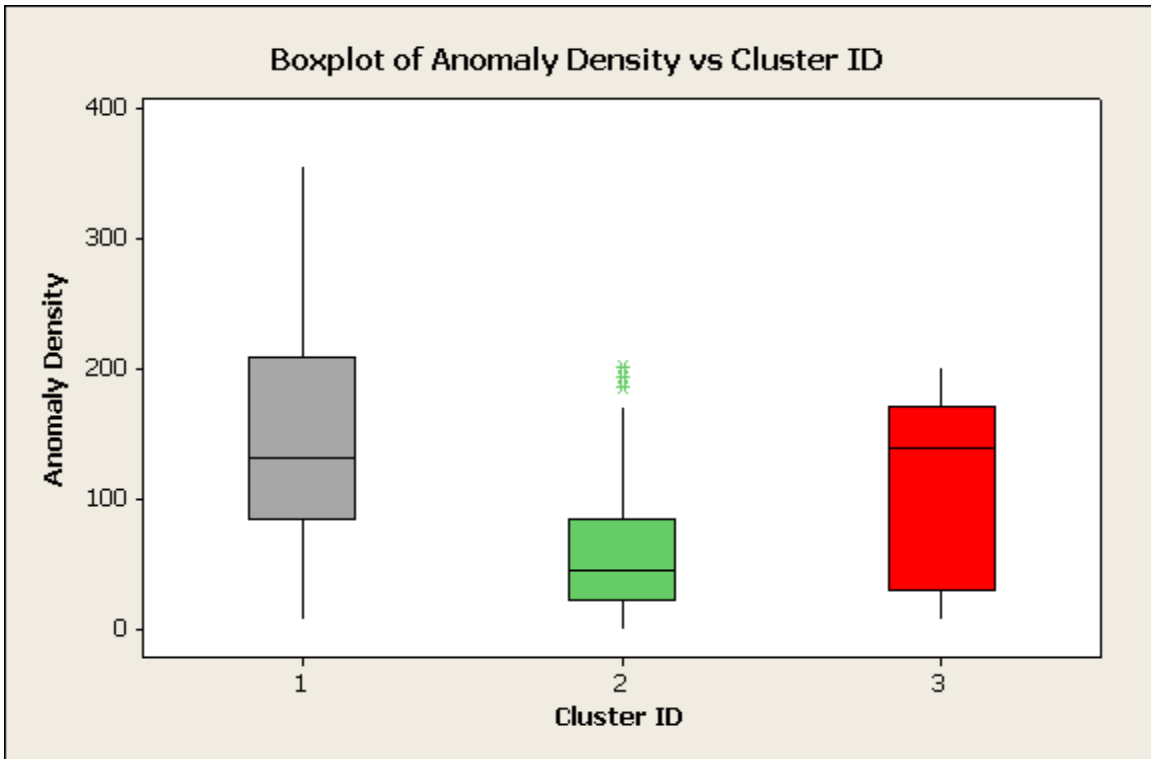
**Figure 32.** Box–and-whisker plots of anomaly density in anomalies per acres (top plot), and outcrop distance in meters (bottom plot) for each group resulting from the K-means cluster analysis. The color scheme matches that used in Figure 30.

38

**Table 3.** Descriptive statistics by cluster ID for each of three clustering variables. The IQR column presents the inter-quartile range.

| Statistics for Cluster Variables | | | | | |
|---|---|---|---|---|---|
| Cluster | Mean | IQR | Min | Max | N |
| Analytic Signal Value (nT/m) | | | | | |
| 1 | 130.7 | 57.6 | 62.6 | 1734.1 | 809 |
| 2 | 190.6 | 119.9 | 62.5 | 1431.3 | 1062 |
| 3 | 2757.8 | 1430.5 | 1398.3 | 10494.3 | 36 |
| | | | | | |
| Anomaly Density (ApA) | | | | | |
| 1 | 146.7 | 124.0 | 8.1 | 357.2 | 809 |
| 2 | 57.2 | 62.1 | 0.0 | 202.2 | 1062 |
| 3 | 114.5 | 140.7 | 7.7 | 202.1 | 36 |
| | | | | | |
| Outcrop Distance (m) | | | | | |
| 1 | 368.0 | 300.4 | 0.0 | 970.3 | 809 |
| 2 | 1081.4 | 556.5 | 203.8 | 2597.5 | 1062 |
| 3 | 1531.6 | 207.3 | 445.8 | 2497.0 | 36 |

## 4.7.2.  Target Area Identification, Delineation, and Density Estimation

To examine the impact of geologic noise in the anomaly data, an additional set of target identification and density estimates were developed excluding those anomalies classified as geologic noise.  Based on the K-means cluster analysis presented above, those anomalies classified as Group 1 most likely represent geologic noise and were removed from the following analyses.

Figure 33 shows the flagged areas of high density based on a 300-m-diameter window and a critical density of 53 ApA.  These values are comparable to those used in the conservative transect design with additional transects (see Figure 19).  As shown in Figure 33, Areas F, G, and I remained unchanged compared to the conservative design with additional transects results.  Areas D, C, H, and J contain no high-density flagging, while Areas A, B, and E show a reduction in flagging.
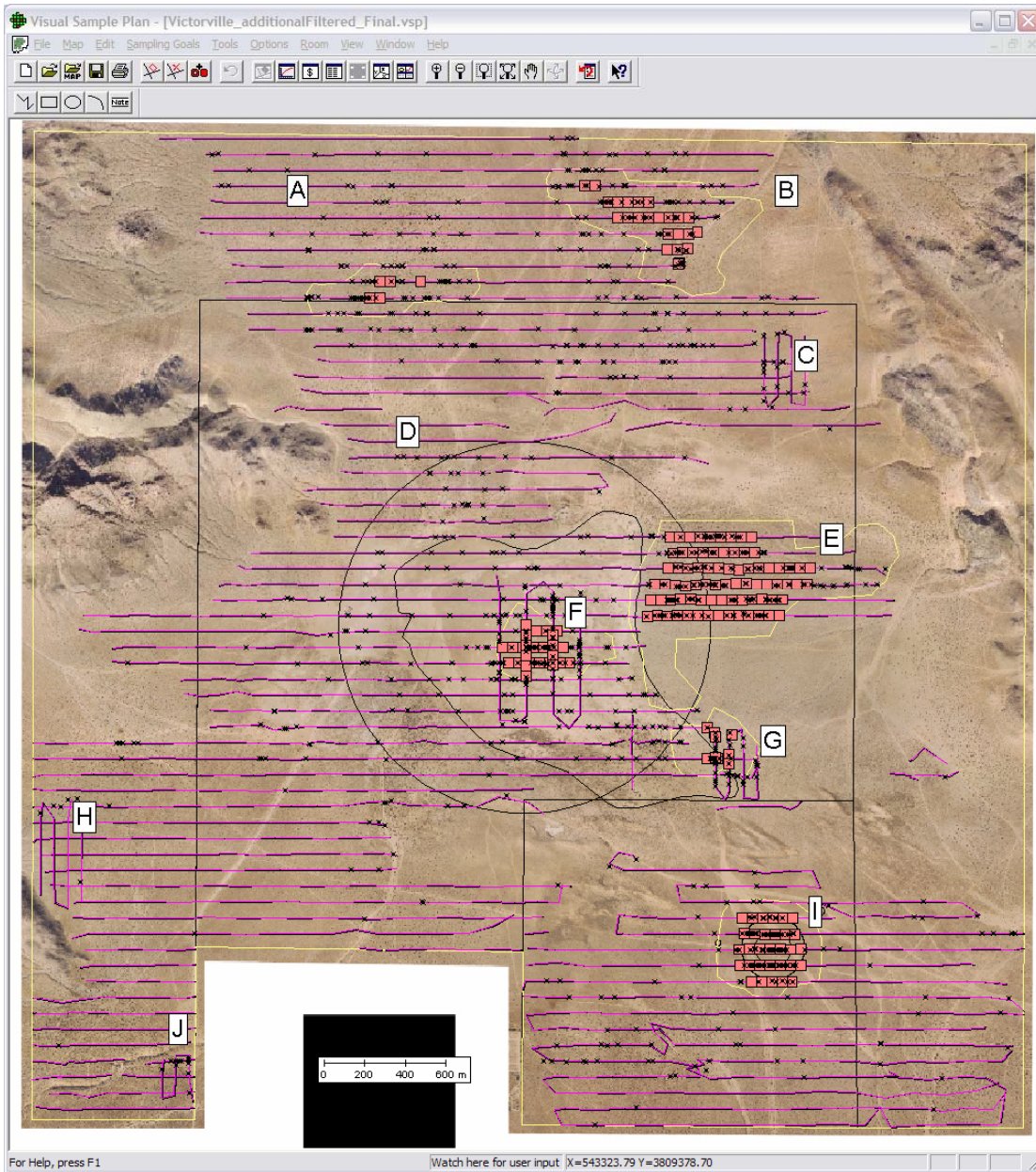
**Figure 33.** Flagged areas of high-density anomalies with a 300-m-diameter window and a critical density of 53 ApA based on the geologically filtered data. High-density-area delineations and site boundaries are depicted with yellow lines.

Figure 34 shows the IK probability levels for the conservative transect design with additional transects after filtering for geologic anomalies using an IK threshold of 53 ApA. Areas with a probability of 0.05 or greater of being above the 53 ApA threshold are indicated by color-filled probability contours. These areas were included as part of the information used in determining the final boundaries for the AOIs.

40

The initial segment (up to 300-m lag) of the semivariogram developed for this data set had a lower slope than that developed for the conservative with additional transects data set. This indicates less spatial variability (greater spatial continuity) for the filtered data set over these distances. Semivariogram parameters are presented in Appendix A.

A comparison of the AOI boundaries in Figure 34 and Figure 20 shows significant differences in many of the AOI delineations. Areas D, C, H, and J were eliminated as AOIs after filtering the anomaly data for geologic noise. In these areas, virtually all of the anomalies from the conservative design with additional transects were classified as Group 1 (geologic noise) during the K-means cluster analysis. Areas A, B, and E show significant reductions in their areas because of the removal of geologic noise. The boundaries for Areas F, G, and I remain unchanged from those designated from the conservative design with additional transects. These areas did not contain any Group 1 anomalies.
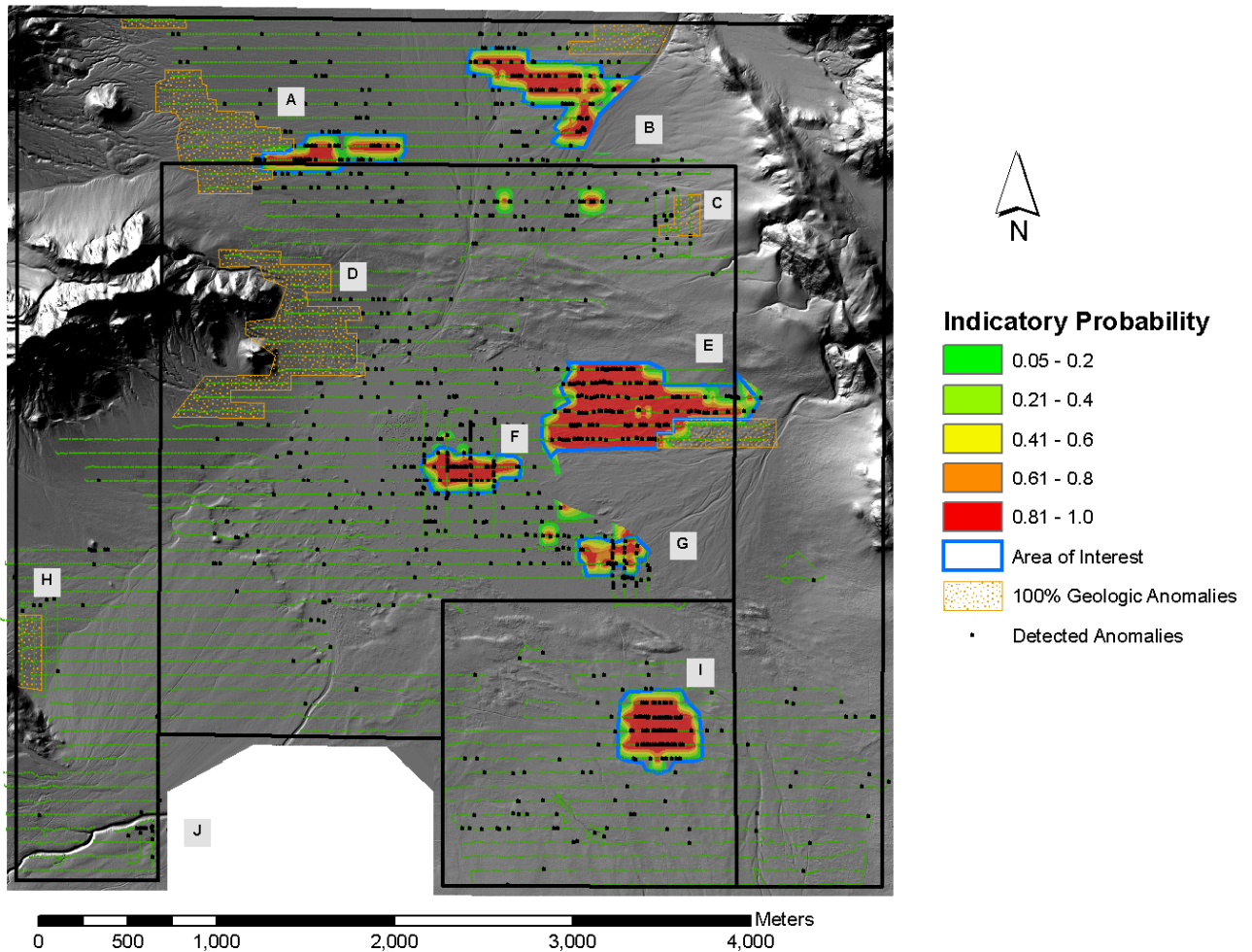


**Figure 34.** Indicator Kriging results and delimited AOIs developed using anomaly data from the Victorville conservative design with additional transects after filtering anomaly data for geologic noise. Brown stippled areas indicate areas of 100 percent anomaly removal from the geologic noise filtering process.

41

Figure 35 shows kriged estimates of anomaly density developed from the geologic filtered anomaly data. This estimate was developed using the transect-based, average anomaly concentrations. The averaging window was 300 m by 100 m and oriented with its long axis in the east-west direction. As in the previously presented density estimates, these estimates were developed using OK with a 20-by-20-m grid cell. A semivariogram model specific to this data set was developed for use in the OK. The parameters for this model did not differ greatly from those for the conservative with additional transects design model. The color-filled contours in Figure 35 indicate anomaly densities; areas without a color overlay have estimated densities below 20 APA. As shown in this figure, the identified AOIs enclose the highest anomaly density locations and correspond with the IK results presented above. It should be noted that if a target area were nestled up against an rock outcropping, this method may have a tendency to classify it as geologic noise, excluding it from target area designation.
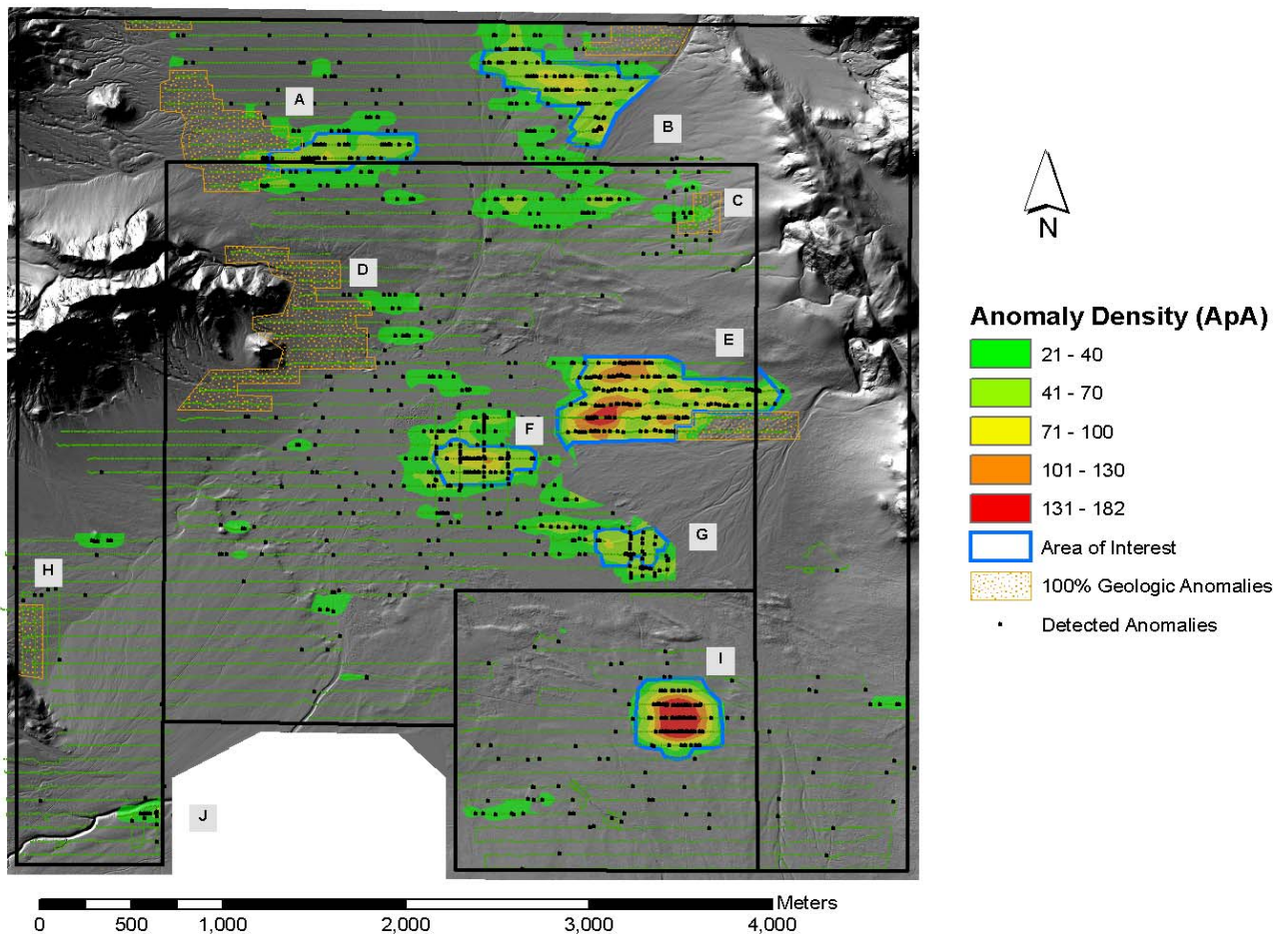


**Figure 35.** Density map of the Victorville conservative design with additional transects based on kriging results after filtering anomaly data for geologic noise. Brown stippled areas indicate areas of 100 percent anomaly removal from the geologic noise filtering process. Blue polygons denote the AOIs determined using IK.

## 4.8. Victorville EMI Supplemental Transect Survey

Subsequent to the initial towed-array magnetometer surveys, and the initial draft of this report, man-carried, EMI survey transects were collected at the Victorville site. These additional surveys were conducted to fill gaps in the initial surveys and to address the issue of local geologic noise. The EMI system is much less susceptible to geologic noise than the magnetometer system and the gathered data was extremely beneficial for eliminating the significant geologic noise component. Although it would be desirable to directly combine the EMI and magnetometer survey data and perform a single flagging and kriging analysis, because these two different sensor systems have different fundamental characteristics (transect width, geologic noise sensitivity, etc.), special consideration is required to interpret these data in combination.

Of the differences between the magnetometer and EMI systems, sensitivity to geologic noise creates the greatest challenge in the combined data evaluation. Because the magnetometer system is much more sensitive to geologic noise than the EMI system, in places where geologic noise is prominent, there is a large difference in the anomalies detected by each system. Figure 36 shows an area of the Victorville site with a large amount of geologic noise. As seen in this figure, there are a series of east-west magnetometer transects that are straddled by EMI transects to the north and south. Although the total north-south distance between the two EMI survey areas is only about 500 m, there is a large difference in the number of detected anomalies between these survey areas and the intervening magnetometer survey area. This difference is highlighted by an abrupt transition in anomaly counts between the different survey areas. This result indicates that the magnetometer surveys were detecting local geologic noise while the EMI surveys were virtually immune to this noise.

In addition to the differences in geologic noise sensitivity, the magnetometer and EMI systems have differing transect widths and spatial resolutions. The EMI system uses one sensor coil to cover a one-meter-wide transects. The towed-array magnetometer system uses a series of eight magnetometer sensors spaced linearly in a cross-track orientation. These sensor configuration differences result in increased cross-track resolution for the magnetometer system.

The result of the system differences discussed above is that a direct analysis of the combined data sets in areas of significant geologic noise is not possible. Because of this issue, the EMI survey analyses will be presented independently.
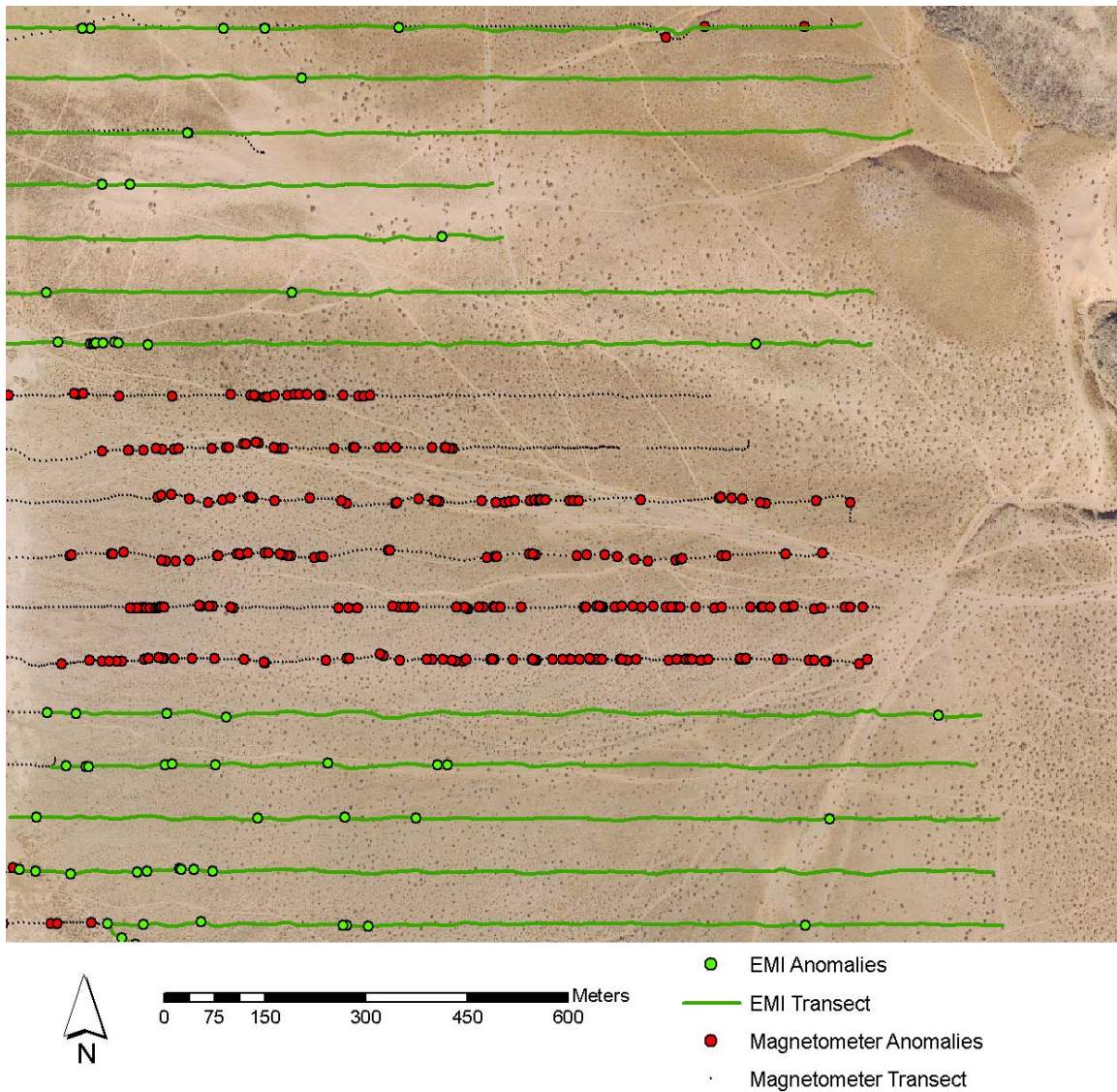
**Figure 36.** Comparison of relative magnetic anomaly counts between the magnetometer and EMI systems in an area of relatively high geologic noise.

As discussed previously, fundamental differences between the magnetometer and EMI survey data preclude directly combining their results. Instead, the EMI survey results will be presented independently here, but will be compared and contrasted with the results from the magnetometer surveys. In general, the EMI survey results corroborate target identification based on magnetometer surveys, and when contrasted against the magnetometer surveys, they confirm the presence of geologic noise in the survey area.

Even in areas without geologic noise, differences in the operational principles between the EMI and magnetometer systems, can generate differences in the survey results from the two systems for the same transect locations. Transformation parameters to allow scaling of the EMI data to more closely match the magnetometer data have been developed for areas with overlapping data (ESTCP 2006b). These transformation parameters were developed by the geophysical survey and processing team based on

comparisons of magnetometer and EMI data at coincident locations. These transformations provide a means of adjusting the EMI data so they more closely match the magnetometer surveys. The applicability of these transformations may be limited in areas of significant geologic noise.

The first transformation is a scaling of the anomaly selection threshold. This is a selection criteria used to segregate the geophysical signal data. Signal values above the threshold are considered magnetic anomalies of interest; those below are considered noise. It is suggested that a scaling factor of 10 should be applied to the EMI cut-off threshold to more closely match the magnetometer data cut-off threshold (ESTCP 2006b). The magnetometer surveys used a threshold value of 62.5 nT/m. This implies a corresponding threshold of 6.25 mV for the EMI data. The original EMI data provided to PNNL and SNL had a cut-off threshold of 4 mV. To more closely match the magnetometer threshold value, the EMI survey data were filtered to remove anomalies with values below 6.25 mV. The resulting data set should reflect anomalies chosen at approximately the same cut-off value as the magnetometer data. It is this data set that is used for results presented here. In addition to the scaling of the anomaly threshold value, it is also suggested that the resulting densities computed from the EMI survey data be scaled by a factor of 0.67 (ESTCP 2006b). This factor will be applied to all the EMI density values and data discussed in the following sections to more closely match the results from the magnetometer surveys.

The EMI transects were spaced according to the conservative transect design (i.e., 78 m) detailed in Section 4.1. However, the transects were surveyed with a 1-m-wide, man-portable EMI system. Figure 37 shows the EMI transects and associated anomalies. Figure 38 shows all the survey transects and anomalies identified at the Victorville site. Both figures show the improved site coverage. A single EMI transect was also collected along a small drainage in the southwest corner of the study area. The majority of this single transect was excluded from these analyses because its isolated nature precluded meaningful analysis and interpretation. The green region (762 acres) identifies the improvement in accessible area on the site and the reduction in inaccessible areas (orange region). These additional transects improved the accessible area to 4229 acres (yellow and green areas), and the additional surveyed transects increased the coverage to approximately 103 acres (2.44 percent coverage).
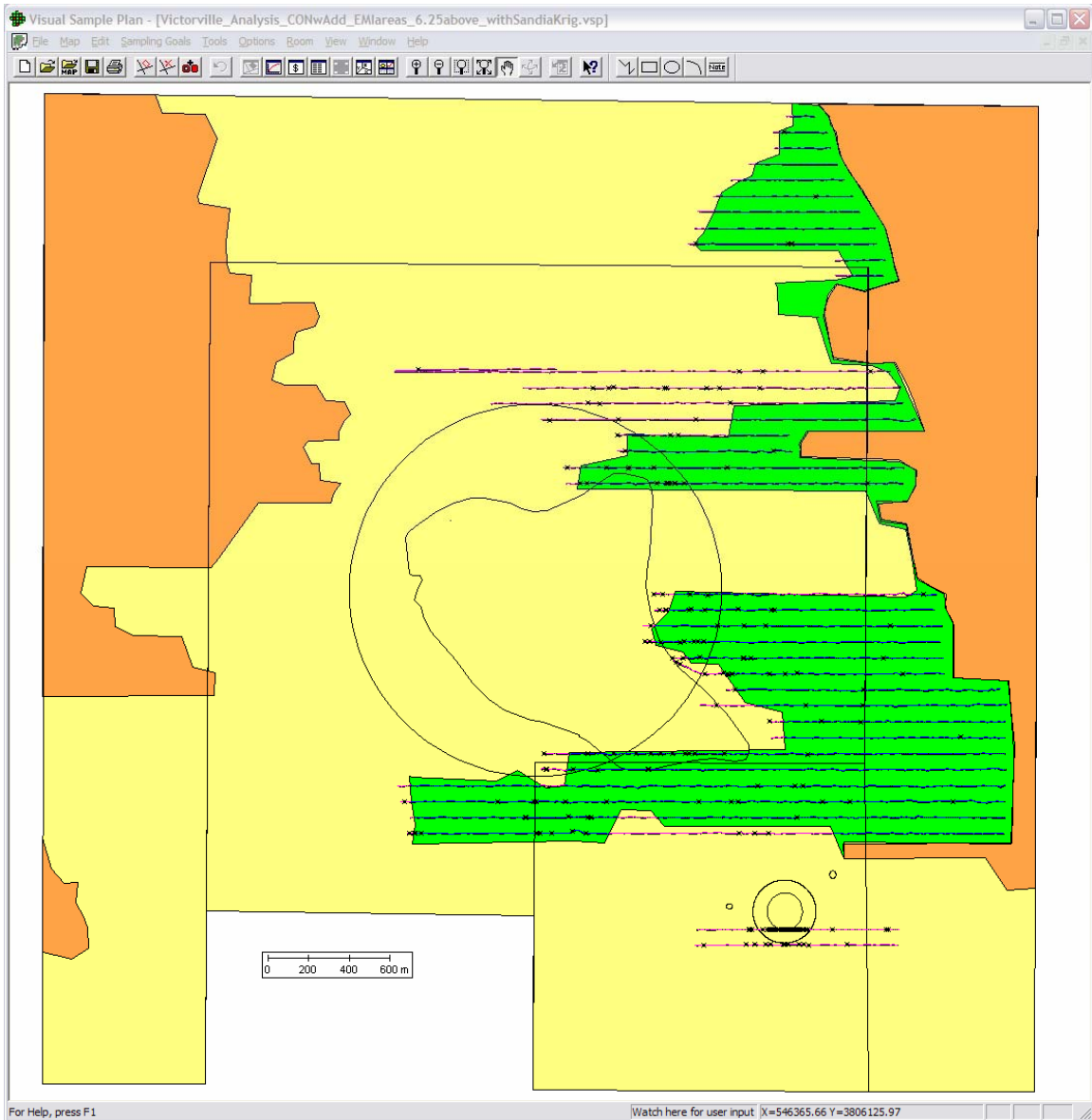
**Figure 37.** EMI transects with anomalies. The orange areas represent the inaccessible regions based on all the surveyed transects (EMI and magnetometer). The green area depicts the reduction in inaccessible area by using the manned-portable EMI system.
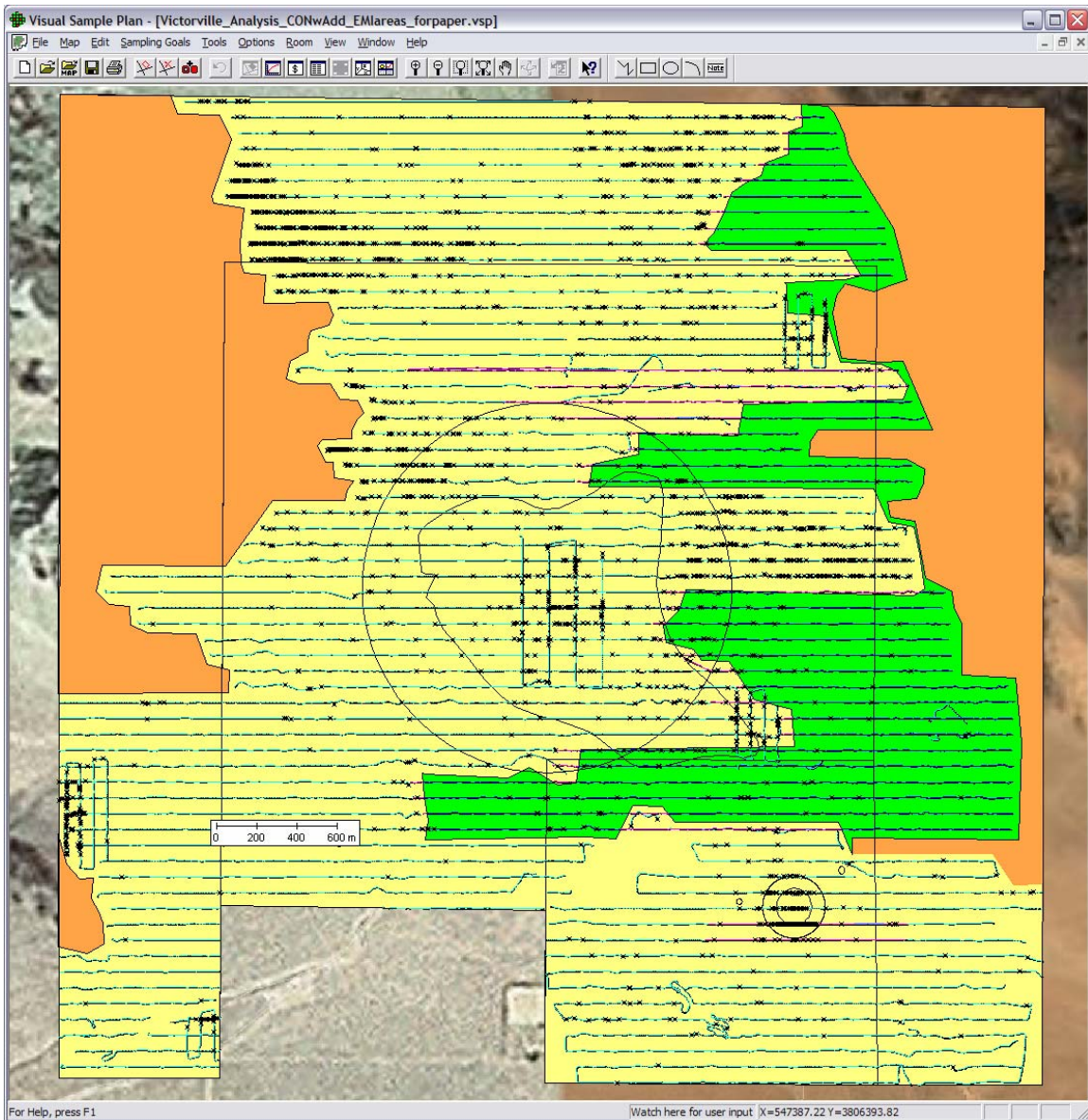
**Figure 38.** All transects and associated anomalies. The orange areas represent the inaccessible regions based on all the surveyed transects (EMI and magnetometer). The green area depicts the reduction in inaccessible area by using the manned-portable EMI system.

### 4.8.1. Target Area Identification, Delineation, and Density Estimation

Figure 39 shows the flagged areas of high density based on a 300-m-diameter window and a critical density of 47 ApA for the EMI transects. There are two isolated flags between AOIs I and M. One flag corresponded with a region identified by the IK estimates shown in Figure 40, and the other isolated flag was not included as an identified AOI. While AOIs K through M lie near AOIs E and G, they were delineated as separate areas because of the differences in sampling technologies and the limited overlap. The locations and sizes of AOIs K through M may imply that the edges of AOIs E and G near the dry lake bed are munitions-related.

47
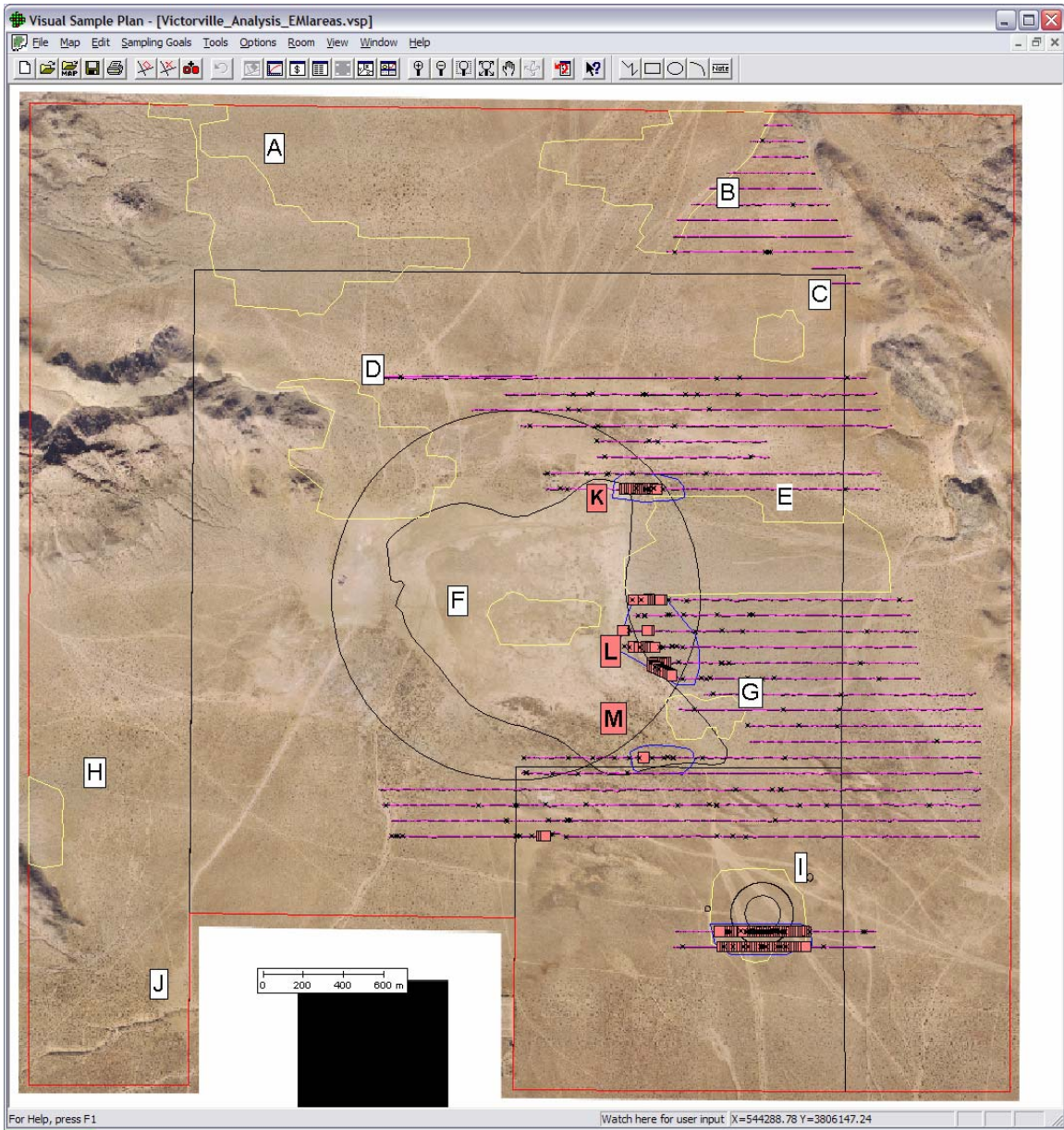
**Figure 39.** Flagged areas based on a 300-m-diameter window and 47-ApA critical density. The regions encompassed by yellow lines (A through J) are previously identified AOIs. Areas K through M are new AOIs from the EMI survey (blue lines). The EMI transects that fell in AOI I identified the same area.

Figure 40 shows the IK probability map developed from the EMI survey data using an IK threshold (adjusted) of 47 ApA. Areas with a probability of 0.05 or greater of being above the 47 ApA threshold are indicated by color-filled probability contours. Newly identified AOIs, Areas K, L, and M, are shown with blue outlines and yellow label fields. Areas of interest previously identified from magnetometer surveys, areas A through J, are shown by gray label fields and dashed outlines. The location of previously identified AOI I is confirmed by the results of the IK using the EMI data. As stated previously, the newly identified AOIs, K, L, and M, are adjacent to previously identified AOIs. AOIs K,

48

L, and M may provide information about those parts of AOIs E and G that are a result of high geologic noise. These new EMI-based AOIs are adjacent to the bed of Means Dry Lake and likely represent munitions-related anomalies. The anomalies shown in Figure 40 are the result of filtering to remove anomalies below 6.25 mV as discussed above. The semivariogram model parameters used for the EMI transect data are listed in Appendix A.
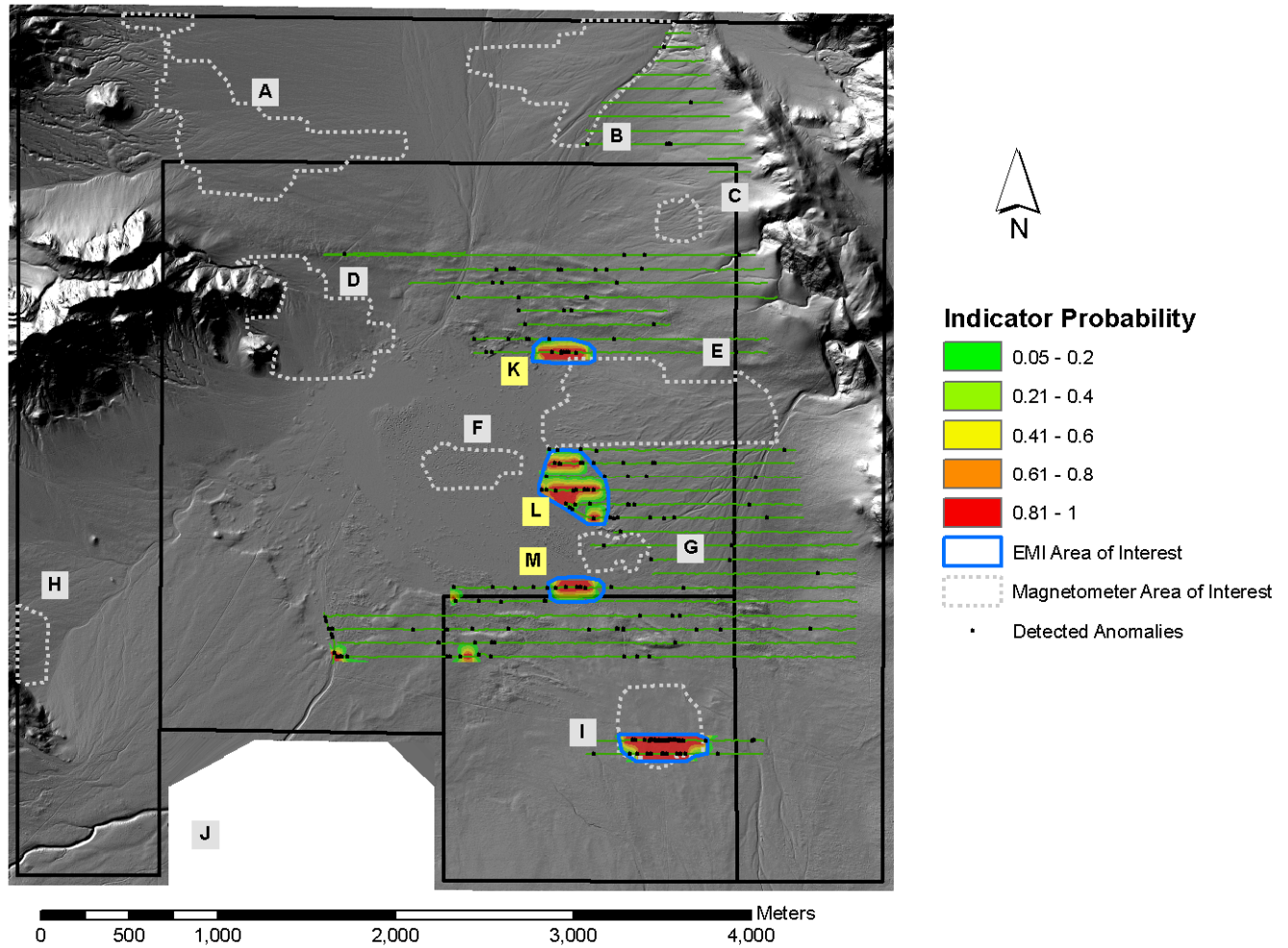


**Figure 40.** Indicator Kriging results and delimited AOIs developed using magnetic anomaly data from the EMI system. Newly identified AOIs are indicated by yellow label fields and blue outlines. Areas of interest identified from magnetometer surveys are shown by gray dashed lines and gray label fields. The EMI survey transect locations are shown by green lines.

Figure 41 shows kriged estimates of anomaly density developed from the EMI transect data. This estimate was developed using the same data set as used in the IK presented above. The averaging window used in the data preprocessing was 300 m by 100 m and oriented with its long axis in the east-west direction. As in the previously presented density estimates these estimates were developed with OK using a 20 m by 20 m grid cell. A semivariogram model specific to this data set was developed for use in the OK. The parameters for this model are listed in Appendix A. The color-filled contours in

Figure 41 indicate anomaly densities; areas without a color overlay have estimated densities below 20 APA.  As shown in this figure, the identified AOIs enclose the high anomaly density locations and correspond with the IK results presented above.  The highest anomaly densities are associated with AOI I.  This is in contrast to the magnetometer survey results where the highest anomaly densities occurred in regions of geologic noise such as AOI A.  This results shows that the EMI system was successful in filtering out local geologic noise.
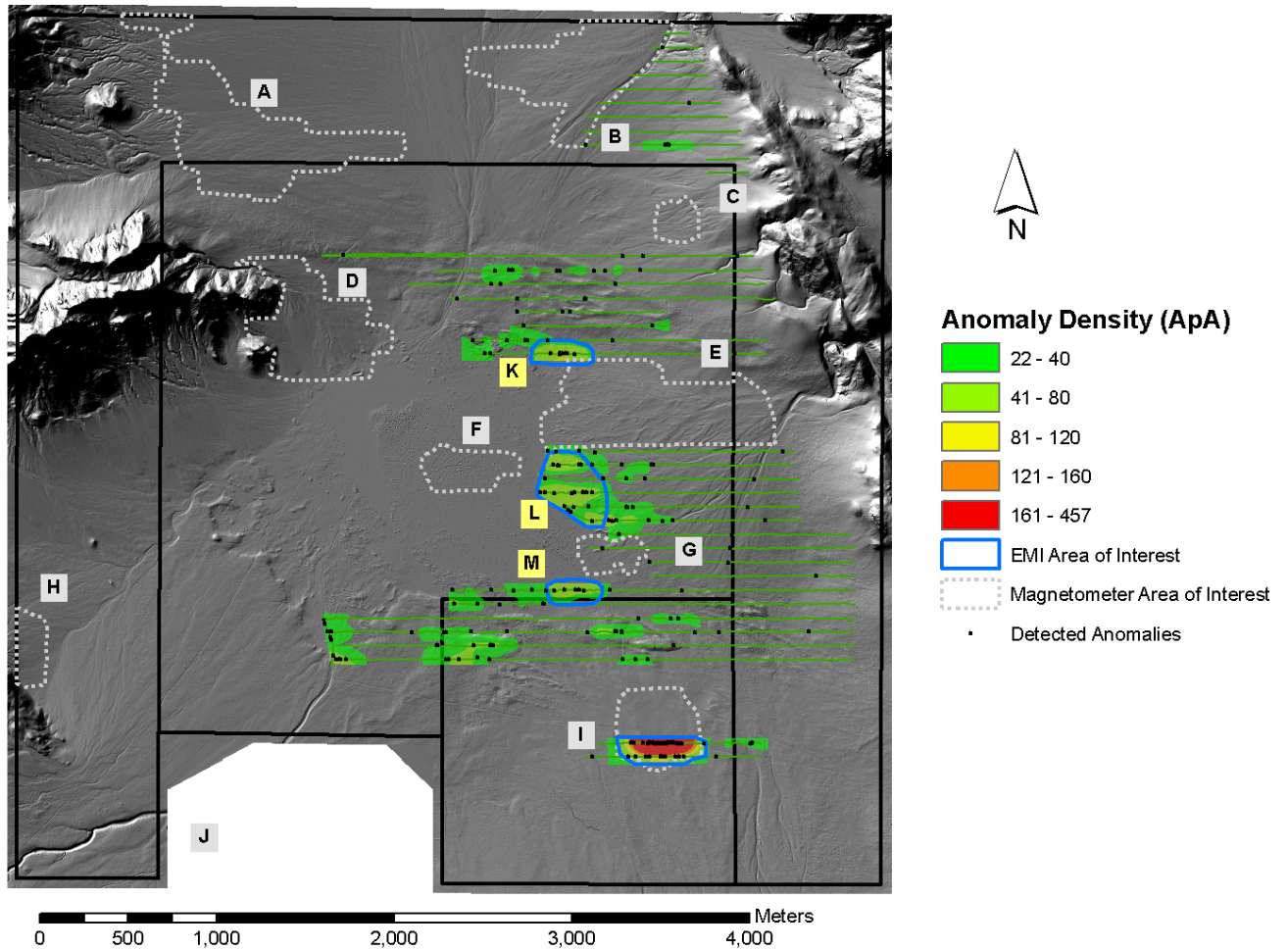


**Figure 41.**  Map of OK estimate of anomaly density created using EMI magnetic anomaly data.  Areas of interest identified from the EMI data are indicated by yellow label fields and blue outlines.  Areas of interest identified from magnetometer surveys are shown by gray dashed lines and gray label fields.  The EMI survey transect locations are shown by green lines.

The results from the EMI transect surveys provide significant information regarding two aspects of the Victorville site. Of primary interest is the identification of three new AOIs (Areas K, L, and M) that are likely related to munitions use in and around the Means Dry Lake bed area. The EMI survey data also provide additional confirmation regarding AOI I, which was initially identified from the magnetometer survey data and for which there is corroborative ground surface evidence of munitions range activities.

In addition to the delineation and confirmation of AOIs, the EMI survey data also provide important evidence substantiating concerns regarding geologic noise at the Victorville site. As shown in Figure 36 adjacent transects from the magnetometer and EMI systems show dramatically different results. The large number of anomalies identified by the magnetometer system in Figure 36 is attributable to magnetically active alluvial rock material from local rock outcrops. This indicates that some of the high anomaly density areas identified in the magnetometer surveys represent geologic noise. In addition, as part of the EMI survey, two areas suspected of containing magnetically active geologic materials were surveyed with the EMI instrument using 100 percent coverage (ESTCP 2006b). Each of these 100 percent coverage areas were approximately 1 acre in size. For the first area (Hot #1), which was located in AOI A, no magnetic anomalies were identified in the EMI survey results. For the second area (Hot #2), located in AOI B, only one anomaly was identified in the EMI survey results. These results corroborate the geologic anomaly filtering analysis presented in Section 4.7.1, and indicate that AOI A and B are likely due to geologic noise and not related to site munitions use.

With the confirmation of geologic noise in the magnetometer survey results, it is likely that other AOIs delineated from the magnetometer surveys may be primarily the result of this noise and not actually related to munitions use at the site. In particular, AOIs C, D, E, G, and H also are likely the result of magnetic anomalies associated with local geology and not with historic munitions use at the site. This conclusion is based on examination of the EMI survey data, the cluster analysis presented in Section 4.7.1, and the LIDAR terrain data. However some possible crater-like features were noted in the LIDAR data for Area D. The remaining AOIs, Areas F, I, K, L, and M, are those most likely associated with historic munitions use at the site. Area J was previously eliminated as an AOI based on the results of additional transect data (see Section 4.4.1).

# 5. Summary and Proposals

## 5.1. Summary of Transect Designs and Target Area Assessment

Statistically based site characterization tools have been successfully applied to the Victorville Precision Bombing Range as part of an assessment of technologies applicable in the wide-area characterization of UXO sites. Application of these tools has provided an efficient and defensible characterization of the Victorville site. Highlights of these results include:

- Development of transect designs that provide 100 percent probability of traversing the target area size and shape identified in the conceptual model and had a high probability of detecting the target area size and shape agreed upon by the design meeting members. This transect design only required that 2.57 percent of the site be surveyed (1.3 percent for the sparse design).
- Identification of multiple distinct AOIs across the Victorville site.
- Probabilistic delineation of all AOI boundaries and estimation of geophysical anomaly density within each identified target area.
- Spatial classification of geophysical anomalies into groups that are more-or-less indicative of geologic noise.
- Quantitative comparison of original magnetometer survey results with follow-on EMI survey to confirm presence of geologic noise and eliminate some AOIs from further consideration.

Details on these different results are provided below along with a summary of the results for different design parameters considered.

Characterization of the Victorville site was accomplished using two geophysical transect designs. The first design was selected by the design meeting members based on the different ordnance previously used at the site. This design had a 100 percent probability of traversing any target area larger than 250 ft in diameter and had approximately 99 percent probability of detecting any 500-ft-diameter target area with a density at the target edge of 8 APA above the assumed background of 8 ApA. The traversal requirement of this design is especially conservative in that no account for an increase in the size of the target area because of fragmentation of the exploded ordnance was considered. Analysis of the geophysical transect data from this conservative design identified 10 different potential target areas. For all 10 target areas, both target area boundaries and anomaly density estimates within the target area boundaries are estimated. Additional transects were collected and used to refine the flagging, boundary, and density estimates. This analysis resulted in the removal of one of the areas from consideration as a target area.

52

A second conceptual model was considered and resulted in a geophysical survey requiring one-half of the original transects in the conservative design. This design had greater then 90 percent probability of detecting a 500-ft-diameter target area with a density at the target edge of 60 ApA above the background of 8 ApA. These transects were analyzed and the flagged regions, the target area boundaries and the anomaly density within the target regions were recalculated. Table 4 compares the results of theses estimations made using the original conservative transect design with the results made using the less conservative sparse design.

The data collected in the conservative design with additional transects were reanalyzed using a filtering procedure based on multivariate clustering. This filtering process was developed to try and remove geologic noise that could be interpreted as geophysical anomalies associated with previous ordnance operations. The results of using the filtered data set are also compared with the results of the other data sets in Table 4.

**Table 4.** Summary of AOI delineations for all data sets. Estimated Anomalies columns present the expected number of anomalies contained within that AOI boundary. Dashes (-) indicate that an AOI was not delineated using that data set.

| AOI | Conservative Design | | Conservative+Additional | | Sparse Design | | Filtered Data Set | |
|---|---|---|---|---|---|---|---|---|
| | Area ($m^2$) | Estimated Anomalies | Area ($m^2$) | Estimated Anomalies | Area ($m^2$) | Estimated Anomalies | Area ($m^2$) | Estimated Anomalies |
| A | 549,600 | 16,409 | 539,200 | 16,367 | 563,200 | 16,047 | 120,800 | 1,525 |
| B | 394,800 | 6,060 | 396,400 | 6,038 | 364,400 | 5,371 | 229,200 | 2,982 |
| C | 39,200 | 537 | 48,400 | 841 | - | - | - | - |
| D | 350,800 | 6,733 | 344,400 | 6,701 | 344,000 | 6,683 | - | - |
| E | 508,000 | 11,355 | 508,000 | 11,515 | 510,800 | 10,583 | 395,600 | 7,445 |
| F | 109,600 | 1,576 | 106,000 | 1,625 | 166,000 | 2,275 | 106,000 | 1,623 |
| G | 51,600 | 585 | 67,600 | 880 | 109,600 | 1,152 | 67,600 | 877 |
| H | 75,200 | 1,323 | 68,000 | 1,403 | 56,400 | 771 | - | - |
| I | 183,200 | 3,800 | 184,400 | 3,816 | 216,800 | 4,347 | 183,600 | 3,808 |
| J | 34,800 | 368 | - | - | 68,400 | 686 | - | - |
| Sum | 2,296,800 | 48,746 | 2,262,400 | 49,187 | 2,399,600 | 47,917 | 1,102,800 | 18,261 |

The summaries in Table 4 show that the additional transects added to the original conservative design resulted in a decrease of 1.5 percent in the total area delineated as an AOI. Most of this was the result of the elimination of Area J as an AOI. The total number of anomalies estimated for the entire area increased by only 0.9 percent, indicating some refinement in the anomaly density estimates for some AOI.

Comparing the conservative with additional transects data set with the less conservative sparse data set shows that the estimates of total area delineated as AOI was larger by 6.1 percent and that the total anomaly count was smaller by 2.6 percent for the sparse data set. One AOI area, Area J, which was eliminated as an AOI in the conservative with additional transects data set, was included as an AOI in the results from the sparse design data set. Conversely, AOI C, which was identified in the conservative with additional transects data set, was not flagged in the sparse transect data set. Area of interest C was the smallest AOI in the conservative with additional transects data set, and many of the anomalies associated with it are likely local geologic noise (see Figure 30).

The last two columns of Table 4 show characteristics for the AOI delineated using only the anomaly data not believed to be the result of geologic noise as determined by the K-means cluster analysis. Results from the filtered data set identified six individual AOIs. This is reduced from the nine AOI identified in the original conservative with additional transects data set. The total area of the AOIs and the total anomaly count were reduced by 51.3 percent and 62.9 percent, respectively, compared to the original data set. If the anomaly data filtered via the K-means cluster analysis are in fact the result of local geologic factors, then these results represent a significant reduction in the areas requiring further investigation. It should be noted that if target areas were nestled up against rock outcroppings, this method may have a tendency to classify it as geologic noise, excluding it from target area designation.

Based on Figure 34 and Figure 35, and the summary results listed in Table 4, it appears that the anomalies associated with AOIs C, D, and H are most likely the result of geologic noise. The anomalies associated with AOIs A and B are potentially related to geologic noise. Areas of interest E, F, G, and I remain as large, high-anomaly-density areas after the filtering process. These areas have the highest potential to contain materials related to former munitions use at the Victorville site and AOIs E, F, and I do correspond to target areas identified by the CSM.

The summary discussion above is based on the results from the magnetometer survey data. Subsequent to this initial survey and the initial draft of this report, EMI survey transects were collected at the Victorville site. These surveys were conducted to fill gaps in the initial magnetometer survey transects and to address the issue of geologic noise. Because of fundamental differences in the two geophysical survey systems (EMI and magnetometer) and the presence of geologic noise in the magnetometer surveys, it was not possible to directly combine the results from both surveys. Instead, the EMI survey data were analyzed separately, and the results were compared to those from the magnetometer survey data. These results confirm the existence of geologic noise in the magnetometer surveys, and indicate that several of the AOIs identified from the magnetometer data are most likely the result of geologic factors.

Based on examination of the EMI survey data and the cluster analysis presented in Section 4.7.1, it is likely that several of the identified AOIs are the result of magnetic anomalies associated with local geology and not with historic munitions use at the Victorville site. The collection of 100 percent coverage EMI data within AOIs A and B confirm that these areas represent geologic noise in the magnetometer survey data. The K-means cluster analysis presented in Section 4.7.1 identified AOIs A, B, C, D, and H as being areas likely or potentially the result of geologic noise in the magnetometer transect data. The examination of magnetometer and EMI survey transects in and around AOIs E and G suggests that these AOIs are likely a combination of geologic noise and munitions-related items. Area of interest J was previously eliminated as an area of concern through the collection additional transect data (see Section 4.4.1). The remaining AOIs, Areas F, I, K, L, and M are those most likely associated with historic munitions use at the site. The total area of AOIs F, I, K, L, and M is about 490,000 $m^2$. This represents only 22 percent

of the total of all the AOIs identified from the towed magnetometer array survey indicating the major impact of the local geologic material.

## 5.2.    Proposals for Future Analyses

The Victorville site is the first WAA site to present significant amounts of geologic noise that must be dealt with in the analysis of the geophysical anomaly data.  While this current analysis presents a means of filtering geologic noise, it will require rigorous validation.  This validation can be done by comparison with additional geophysical or other types of information collected at the site.  This additional information may assist in determining the accuracy of the K-means cluster analysis; in particular, it may aid in determining the accuracy of the geologic-noise group determination.  In the future, if high density anomaly areas covered by magnetometer surveys that are suspect of containing significant geological noise can be augmented with EMI surveys over those same high-density areas, a more direct comparison and set of adjustment factors might be feasible.

The 100 percent coverage provided by the helicopter data will provide another feature that could be used in the multivariate clustering.  This feature is the nearest-neighbor distance between anomalies, which may show differences between geophysical anomalies of geologic and anthropogenic origin.  The nearest-neighbor distance cannot be determined from limited transect data, but can be calculated from data collected with 100 percent coverage.  Comparison of the 100 percent coverage helicopter and 100 percent ground-based geophysical data may also provide insight into the origins of some of the suspect high anomaly density areas.

# 6. References

Davis JC. 1986. *Statistics and Data Analysis in Geology*. John Wiley and Sons, New York.

Environmental Security Technology Certification Program (ESTCP). 2006a. *WAA Pilot Project Data Report – Wide Area UXO Contamination Evaluation by Transect Magnetometer Surveys, Victorville Precision Bombing Ranges Y and 15*. ESTCP Project # MM-0533, May 3, 2006, Washington, D.C.

Environmental Security Technology Certification Program (ESTCP). 2006b. *WAA Man-Portable EM Demonstration Data Report, Victorville Precision Bombing Ranges Y and 15*. ESTCP Project # MM-0533, November 17, 2006, Washington, D.C..

Hassig NL, JE Wilson, RO Gilbert, BA Pulsipher, and LL Nuffer. 2005. *Visual Sample Plan Version 4.0 User's Guide*. PNNL-15247, Pacific Northwest National Laboratory, Richland, Washington.

Matzke BD, JE Wilson, and BA Pulsipher. 2006. *Version 4.4 Visual Sample Plan (VSP): New UXO Module Target Detection Methods*. PNNL-15843, Pacific Northwest National Laboratory, Richland, Washington.

Nova Research. 2006. *Wide Area UXO Contamination Evaluation by Transect Magnetometer Surveys, Victorville Precision Bombing Ranges Y and 15, Victorville, CA 20-31 March 2006*, Washington, D.C..

Roberts CW and RC Jachens. 1999. *Preliminary Aeromagnetic Anomaly Map of California*. USGS Open-File Report 99-440, Washington, D.C. Available at http://geopubs.wr.usgs.gov/open-file/of99-440/of99-440.pdf.

U.S. Department of Agriculture (USDA). 2006. *Partial Soil Survey Geographic (SSURGO) Database for Mohave Desert Area, West Central Part*. Natural Resources Conservation Service, Washington, D.C. Available at http://SoilDataMart.nrcs.usda.gov.

# Appendix A


**Semivariogram Parameters**

This appendix presents the analytical model parameters used during the kriging analyses. Semivariograms from observational data were computed using a lag of 20 m and a lag tolerance of 10 m. Observational data consisted of anomaly densities in anomalies per acre.

**Semivariogram Model Parameters for Density Estimates Developed Using Ordinary Kriging**

| Transect Data Set | Nugget | Model Type[1,2] | Sill[1] | Range[1] (m) |
|---|---|---|---|---|
| Conservative | 0.0 | Gau. / Sph. | 750 / 400 | 630 / 900 |
| Conservative + additional | 0.0 | Gau. / Sph. | 730 / 450 | 630 / 1200 |
| Sparse | 0.0 | Gau. / Sph. | 740 / 700 | 930 / 1400 |
| Geology filtered | 0.0 | Sph. / Gau. | 600 / 600 | 650 / 1070 |
| EMI Survey | 23.6 | Sph. | 1200 | 311 |
| [1] Two nested models were used, parameters for first and second model listed respectively. [2] Spherical model abbreviated Sph; Gaussian model abbreviated Gau. | | | | |

**Semivariogram Model Parameters Used in Indicator Kriging Analyses**

| Transect Data Set | Nugget | Model Type[1,2] | Sill[1] | Range[1] (m) |
|---|---|---|---|---|
| Conservative | 0.0 | Sph. / Exp. | 0.045 / 0.06 | 440 / 1750 |
| Conservative + additional | 0.0 | Sph. / Exp. | 0.05 / 0.06 | 270 / 2000 |
| Sparse | 0.0 | Sph. / Exp. | 0.025 / 0.078 | 350 / 1300 |
| Geology filtered | 0.0 | Sph. / Exp. | 0.038 / 0.078 | 340 / 2000 |
| EMI Survey | 0.0 | Exp. | 0.048 | 540 |
| [1] Two nested models were used, parameters for first and second model listed respectively. [2] Spherical model abbreviated Sph; exponential model abbreviated Exp. | | | | |